

POLITECNICO DI TORINO

Collegio di Ingegneria Meccanica, Aerospaziale, dell'Autoveicolo e della Produzione

**Corso di Laurea Magistrale
in Mechanical Engineering**

Tesi di Laurea Magistrale

Backup bearing test bench upgrade and evaluation



Relatori

firma del relatore (dei relatori)

Prof. Eugenio Brusa

.....

Prof. Petri Kusomanen

Ing. Raine Viitala

Candidato

firma del candidato

Michele Tunesi

“The path of the righteous man is beset on all sides by the iniquities of the selfish and the tyranny of evil men. Blessed is he, who in the name of charity and good will, shepherds the weak through the valley of darkness, for he is truly his brother’s keeper and the finder of lost children. And I will strike down upon thee with great vengeance and furious anger those who would attempt to poison and destroy my brothers. And you will know my name is the Lord when I lay my vengeance upon thee.”

Ezekiel 25:17

Abstract

Safety of the machines and evaluation of backup systems is fundamental for the industry to develop a secure environment for the employee and ensure that components do not get damaged in case of a failure. Having the possibility to test the behavior of a bearing under the extreme stress of a simulated failure scenario is an important capability that allows to practically test these complex components. The test bench aims to characterize the behavior of the shaft when drop down at high speed on a backup bearing set. The machine was developed and designed to have a high rpm speed of test and quick maintenance and calibration.

The aim of the study was to start on the solid design previously done and improve it to extend its capabilities and to fix some of the calibration and operational problems that became evident with time. The system was designed to withstand rpm up to 28'000, and the screw positioning system was fixed to obtain that. The vibration during acceleration were quite large, in the order of the hundreds of μm , and now thanks to the screw system and the lower holder plate modification are reduced in the order of the tens of μm . As a further expansion of the capabilities, a measurement system for the temperature was added on one side of the machine to record the temperature on the outer ring of the bearing.

The main result was that the machine now is capable of reliably perform the tests without interruption and with no need of recalibration between each test. The centering remains stable through the measurement runs. The temperature measurement system is set up and ready to record data. Some initial test showed an interesting gradient of temperature in time toward the higher part of the bearing, exactly on the opposite side of where the shaft is dropped.

Acknowledgements

First of all I would like to thank all the people that allowed me to work on this interesting project for my thesis: professor Petri Kuosmanen for choosing me for this topic, and for the help through the thesis, Raine Viitala and Juuso Autio for all the help in figuring out how to solve the problems, Jouni Pekkarinen and Thomas Widmaier for all the expertise and work in the production of custom pieces, as well as helping me getting a hold of the laboratory. Thanks also to Mattia Vaira for the help during the calibration process as a computer assistant.

I would like also to thank Eugenio Brusa for all the help from Italy during my work, and for the various advices received during this fantastic period here in Finland.

Thanks also to all the friends that made my exchange in Finland a life changing experience. Emanuele, Fabio, Fabrice, Greta, Jenny, Manfredi, Oleg, Rasmus, Sabrina, Valentina and Veera helped me make this period one of the most beautiful and rich in my life. Work and studying is important, but if not shared with the right people it is meaningless.

Thanks to my host in Espoo Helena. She has been a good friend and with Muru and Nana they made Finland feel more like a home than a simple place I lived.

Finally, I would like to thank my family: my mother Marisa, my brother Lorenzo, Piero, Bruno, Marco and my grandparents Liliana and Michele, as well as all the others in my family. It never passed a day where they didn't believe in me and did all they could to let me have this amazing Erasmus.

A special mention to Steve Gunn and Sunil Patel for sharing the L^AT_EX template on which my thesis was written on.

Ringraziamenti

Innanzitutto vorrei ringraziare tutte le persone che mi hanno permesso di lavorare a questo interessante progetto per la mia tesi: il professore Petri Kuosmanen per avermi affidato questo argomento, e per l'aiuto durante la tesi, Raine Viitala e Juuso Autiosalo per avermi dato una mano a risolvere i problemi, Jouni Pekkarinen e Thomas Widmaier per la loro esperienza e per tutto il lavoro nella produzione dei componenti necessari, ma anche per avermi aiutato nel usufruire del laboratorio. Grazie anche a Mattia Vaira per essere stato il mio assistente al computer durante il processo di calibrazione

Vorrei anche ringraziare Eugenio Brusa per l'aiuto dall'Italia durante il mio lavoro, e per tutti i vari consigli ricevuti durante questo fantastico periodo in Finlandia

Grazie di cuore a tutti gli amici che hanno reso il mio scambio in Finlandia un'esperienza che ha cambiato la mia vita. Emanuele, Fabio, Fabrice, Greta, Jenny, Manfredi, Oleg, Rasmus, Sabrina, Valentina e Veera hanno reso questo tempo uno dei più belli e ricchi della mia vita. Lavorare e studiare è importante, ma se non si condivide il tempo con le persone giuste si perde qualsiasi significato.

Grazie alla mia host in Espoo Helena. È stata una vera amica e con Muru e Nana mi ha fatto sentire la Finlandia più una casa che un semplice posto.

Infine vorrei ringraziare la mia famiglia: mia madre Marisa, mio fratello Lorenzo, Piero, Bruno, Marco e i miei nonni Liliana e Michele, come tutti gli altri nella mia famiglia. Non è passato un giorno in cui non abbiano tutti creduto in me e hanno fatto tutto il possibile per permettermi di avere questo fantastico Erasmus.

Un speciale ringraziamento va a Steve Gunn e Sunil Patel, per aver condiviso il template L^AT_EX su cui questa tesi è stata scritta.

Contents

| | |
|--|-------------|
| Abstract | v |
| Acknowledgements | vii |
| Ringraziamenti | ix |
| Contents | xi |
| List of Figures | xiii |
| List of Tables | xv |
| List of Abbreviations | xvii |
| 1 Introduction | 1 |
| 1.1 Background | 1 |
| 1.2 Research problem | 2 |
| 1.3 Aim of the research | 3 |
| 1.4 Scope of the research | 3 |
| 1.5 Research methods | 4 |
| 2 State of the art review | 5 |
| 2.1 Rotor dynamics | 5 |
| 2.2 Bearings | 6 |
| 2.3 Statistics of the normal distribution | 7 |
| 2.4 Temperature measurement theory | 9 |
| 2.4.1 PT-100 temperature sensor | 9 |
| 2.4.2 2-Wire and 3-Wire configuration | 9 |
| 2.4.3 PT-100 calibration process | 11 |
| 3 Research method and equipment | 13 |
| 3.1 AMB ³ test bench working principle and starting setup | 13 |
| 3.1.1 Shaft Assembly | 14 |

| | | |
|----------|--|-----------|
| 3.1.2 | Motor and belt engagement assembly | 15 |
| 3.1.3 | Holder plate engagement assembly | 16 |
| 3.1.4 | Backup bearing support assembly | 16 |
| 3.1.5 | Measurement, data acquisition and control system | 16 |
| 3.1.6 | Data analysis and MATLAB® | 18 |
| 3.1.7 | User interface (UI) | 19 |
| 3.1.8 | Output of the measurement system | 20 |
| 3.2 | Setup procedure and calibration of the machine | 21 |
| 3.3 | Issues with the initial setup | 24 |
| 3.3.1 | Holder plates design | 24 |
| 3.3.2 | Screw design | 25 |
| 3.3.3 | Damaged backup bearings | 26 |
| 3.4 | Temperature measurement introduction | 26 |
| 4 | Results | 29 |
| 4.1 | Vibration analysis | 29 |
| 4.2 | Shaft centering analysis | 31 |
| 4.2.1 | Centering test without the locking nuts | 31 |
| 4.2.2 | Locking system for the screws | 33 |
| 4.2.3 | Centering test with the locking nuts | 34 |
| 4.3 | Backup bearing substitution | 36 |
| 4.4 | Temperature evaluation | 37 |
| 4.4.1 | LabView® and NI system | 37 |
| 4.4.2 | Sensor placement | 40 |
| 4.4.3 | Calibration | 41 |
| 4.4.4 | Measurement results | 41 |
| 5 | Discussion and findings | 45 |
| 5.1 | Centering behavior of the test bench | 45 |
| 5.2 | Temperature behavior of the backup bearings | 47 |
| 6 | Summary | 51 |
| | Bibliography | 53 |
| 1 | Appendix: MATLAB® scripts | 55 |
| 2 | Appendix: Vibration data | 61 |
| 3 | Appendix: Drop down and centering test | 67 |
| 4 | Appendix: Abstract from Aalto University | 73 |

List of Figures

| | | |
|------|--|----|
| 2.1 | Single row high speed ball bearings from SKF 7007CDGAV/HCP4A | 6 |
| 2.2 | 2-Wire configuration schematic. | 9 |
| 2.3 | 3-Wire configuration schematic. | 10 |
| 3.1 | AMB ³ system setup | 14 |
| 3.2 | Belt engaging system (left) and motor assembly (right) | 15 |
| 3.3 | Holder plate assembly in the engaged position | 17 |
| 3.4 | Backup bearing support assembly | 18 |
| 3.5 | Measurement sensors: XY positioning Eddy current sensor (left) and frequency sensor (right) | 19 |
| 3.6 | Java interface to operate the AMB ³ test bench | 20 |
| 3.7 | XY position of the shaft during the measurement run | 21 |
| 3.8 | Speed of the shaft during the drop down | 22 |
| 3.9 | XY positioning and single axis evolution in time | 22 |
| 3.10 | X and Y evolution in time compared with the shaft speed | 23 |
| 3.11 | Modified lower holder plate | 25 |
| 4.1 | Results of the vibration evaluation with 99 % confidence level | 30 |
| 4.2 | Centering test performed at 15000 rpm without the locking screws | 32 |
| 4.3 | Centering test performed at 15000 rpm after the failed drop down test | 33 |
| 4.4 | Detail of the positioning of the locking nuts on the positioning screws | 34 |
| 4.5 | First centering test performed at 15000 rpm with the locking screws | 35 |
| 4.6 | First drop down test at 28000 rpm with the locking screws | 35 |
| 4.7 | Second centering test performed at 15000 rpm with the locking screws | 35 |
| 4.8 | Centering test 2, 3, 4 and 5 with locking nuts | 36 |
| 4.9 | Measurement setup with the NI system | 38 |
| 4.10 | LabView [®] interface to operate the measurement system | 39 |
| 4.11 | LabView [®] program which controls the sensor operation | 39 |
| 4.12 | Detail of the resistance-temperature conversion in LabView [®] code . | 40 |

| | | |
|------|--|----|
| 4.13 | Temperature of the 7 points measured during a full drop down test from a cold machine | 42 |
| 4.14 | Temperature evolution during the heating phase | 43 |
| 4.15 | Temperature evolution during the heating phase | 44 |
| 4.16 | Temperature evolution during the drop down and cooling phase | 44 |
| 5.1 | X-axis and Y-axis extremes for each centering test | 46 |

List of Tables

| | | |
|-----|--|----|
| 2.1 | Probability chart for various Z values (Most commonly used for statistical analysis in bold) | 8 |
| 4.1 | Results of the calibration test | 41 |
| 5.1 | X-axis and Y-axis extremes for each centering test | 45 |
| 5.2 | Temperature change from start to drop down, without and with preheating | 47 |
| 5.3 | Temperature change from drop down to maximum temperature, without and with preheating | 48 |

List of Abbreviations

| | |
|------------------------|---|
| ABB | A SEA B rown B overi |
| AMB³ | A ctive M agnetic B earing |
| CAD | C omputer- A ided D esign |
| CL | C onfidence L evel |
| DOF | D egree O f F reedom |
| NI | N ational I nstruments |
| PTFE | P oly T etra F luoro E thylene |
| rpm | round p er m inute |
| RTD | R esistance T emperature D etector |
| SKF | S venska K ullager F abriken (A B) |
| UI | U ser I nterface |
| VI | V irtual I nstrumentation |

Chapter 1

Introduction

In this chapter the main objects, as well as the main motives of the thesis are presented, with

1.1 Background

The operational safety of large machines has become a common practice in the modern industrial scenario. Country regulation and standard requirement had the effect, in the previous decades, of making the industry environment more capable of preventing, in most cases, failure of mechanical structures, while in other to develop solutions to control the failure of a component.

In the rotor field this innovation has come in the form of more accurate fatigue sizing of the bearings, emergency brakes and backup systems. The latter case is the field of interest of this thesis. In fact, even if the fatigue sizing is done properly, and the inspection schedule is complied, there is always a chance that the primary bearing set could suddenly fail due to an unexpected overload or a non-noticed damage to the components. In this scenario there is the risk of harm to nearby operators and damage to the expansive components around the rotating part.

The backup bearing solution aims to solve this problem. It consists in a set of bearings positioned along the shaft, or rotor, and not in contact during normal work of the machine. Commonly there is a clearance of 0.25 mm between the bearing and the shaft. In case of a failure, the shaft falls on the backup bearing set, that catches it and allows a controlled deceleration, avoiding potential risks to the nearby machinery or workers.

The bearing is one of the fundamental mechanical elements which allows to apply some constraints to a rotating body. There are several types of bearings, depending on the internal specification of the rotating elements, but in general they fix the center of rotation of the section in a point, or a small area in case of bearings with clearance. The main important components of a bearing are the inner and outer ring and the rotating element (in the simplest case a ball bearing). The inner ring is in contact with the rotating body, while the outer ring is in contact with the frame or the structure of the machine. Depending on the design it is possible to constrain any type of linear movement, as well as rotation.

Even if bearings are extremely available on the market, frequent replacement is not an option due to the cost of manufacturing. So extra precautions must be used to properly size the bearings and to avoid unwanted loads that could drastically reduce the fatigue life.

1.2 Research problem

Rotor centering during operation is a fundamental feature of any rotating system. The relative position of the rotor axis with respect to the axis of rotation is one of the factors that leads to the generation of strong vibration and displacement of the rotor itself. For this reason, during the setup, it is important to fix the constraints in the best possible position.

The vibration of the rotor creates an additional periodic load on the bearings, which suffer a non-negligible life shortening due to the stress applied by a fast rotor. Since the AMB³ test bench was designed and assembled to undergo quick tests on different backup bearings [1], the damage of the primary bearing set could lead to an economic cost that lowers the usability of the machine from the economical point of view.

As received, the test bench is only capable of evaluating the center position and to actuate the drop of the rotor on the backup bearings, as well as record the speed of rotation and to be controlled with wireless commands. There is still room for improvement in the range of possible measurements that can be performed on both the bearings and the rotating mass.

1.3 Aim of the research

In the present master thesis study, the interest is focused on the improvement of the existing AMB³ test bench previously built. The test bench is a custom-built machine that allows to accelerate a shaft held by primary bearings, and to simulate the primary bearing failure to test the behavior of the backup bearings. Even if the machine is working as expected with the previous design, some improvements are beneficial to the quality of the tests performed on the bench.

The first problem to be targeted is the positioning and centering of the shaft before the failure simulation. In the current setup, when the holder plate is keeping the shaft controlled by the primary bearing, the center position of the rotating mass is fluctuating around the order of the hundreds of μm for high rpm loads. A new design should be tested and implemented to reach a smaller order of magnitude, in the tens of μm , which is stable in as the test go through.

The second implementation that could lead to interesting data is the temperature measurement of the backup bearings during the drop down and the consequent deceleration of the rotating shaft. Since the deceleration happens almost exclusively due to friction in the bearing set, the thermal evaluation allows to have an energy evaluation of the system. This evaluation will be used to refine the simulation created by the Lappeenranta University of Technology. The temperature measurement setup implies that the whole signal reading system has to be updated or changed.

1.4 Scope of the research

The research presented in this study aims to test and show which improvements are possible on the previously built test bench. It is natural that all the changes are “custom” for the system they are applied to, but some elements could be extendable to similar systems.

The temperature evaluation will be performed with some simplifying assumptions on the heat transfer and heat dissipation phenomena, according to the simulation from Lappeenranta University of Technology.

The research in general will focus on the evaluation of the real experimental results and findings rather than the theory behind each phenomenon. As stated before the aim is to improve the test bench to be more suitable for backup bearing testing.

Even if some programming is required to connect and extract the information from the sensors on the test bench, the aim of this thesis is not to explain how the signal processing works. The program and the electrical configuration will be designed starting from the current setup and further developed.

1.5 Research methods

Starting from the existing AMB³ test bench, the performance of the system in the current disposition is tested and evaluated to have a starting point as a reference. Then, by trial and error steps, the centering system of the holder plate will be corrected to reach the desired threshold for the displacement of the center axis. In the same time, the temperature system is set to operation, and the temperature of the bearings is recorded for the energy evaluation.

The theoretical knowledge used is presented in the Chapter 2, State of the art review, and comprehends a summary of rotor dynamics, bearing sizing, bearing mounting and power transmission, as well as some notions related to signal interpretation from the sensor and temperature measurements theory. In Chapter 3, a complete presentation of the system with a description of the problems is done. In Chapter 4 the results of the modification and solutions applied are shown with some analytical data, and finally discussed in Chapter 5. To conclude this project, a summary is presented in Chapter 6, followed by some Appendices with the more complete data from the various measurements.

Chapter 2

State of the art review

In this chapter some of the basic theoretical remarks are touched in the thesis. The basic concepts are presented and then further inspected if needed, when they are used in the next chapters.

2.1 Rotor dynamics

In the most general definition, rotor dynamics is the science that studies the behavior of a rotor during the rotation, especially to study the vibration modes and the critical speed. The understanding of these components helps to size and to control properly a rotor, as well as to avoid the dangerous speeds. In general, any continuous model of a rotor has a primary resonance frequency where the vibrations are severely amplified, then many others at higher rpm, where the vibrations are also amplified, but with a smaller effect. It is important to evaluate and define these values in order to pass them as quickly as possible during acceleration.

When the rotor presents a simple structure, it is possible to proceed by mathematical analysis. The general method is to associate a general matrix form equation which takes into account acceleration, velocity and displacement vectors, and has to be solved to characterize the properties of the rotor. Some simplifications for the matrix equation are possible, using methods such as lumped parameter models, which concentrates the features of the rotor in discrete entities, or the Rayleigh method, which helps to find the eigenvalues of the equation with the Rayleigh ratio [2].

A common way to evaluate the resonance frequencies is the practical testing of

each speed in order to build a transfer function for each frequency. This method is the most common for complex system where too many components together influence each other in the vibration modes. At each frequency the acceleration obtained by statistical means is considered, in order to assign a specific peak to each speed [3].

2.2 Bearings

The bearings are mechanical elements that allow to constrain some of the DOF of a rotating element. Most common bearings lock all the displacement in the plane of the bearing itself, while allowing a little displacement in the normal direction to the bearing plane. The main task of the bearings is to keep the shaft rotating as stably and as frictionless as possible [4]. Bearings are composed by:

- Outer ring
- Inner ring
- Rolling element
- Bearing cage
- Bearing cap
- Lubricants



FIGURE 2.1: Single row high speed ball bearings from SKF 7007CDGAV/HCP4A

The outer and the inner ring are rigid elements that have a precisely shaped race to accommodate the rolling elements that will be rolling between them.

The rolling elements come in different shapes and with different tasks. The most common shapes are sphere, cylinder, tapered cylinder, needle and cones. Depending on the combination of the race shape and the element shape, the possible constrain limits vary, from fully axial to fully radial.

The cage is a rigid component that locks each rolling element with respect to each other. If not implemented, in some cases, it can lead to the spheres or cylinders to accumulate on one side of the bearing, thus making it not functional and prone to failure. In addition, some kind of lubricant is used to minimize the friction between the rolling elements and all the other components in the bearing. This allows for an efficient rotation that consumes a smaller part of the kinetic energy of the rotating shaft.

Depending on the use case, the bearing must be sized and positioned correctly, otherwise its life span could be diminished by the excessive loads. In the AMB³ test bench, since there is no axial action on the shaft, the bearings are all with spherical rolling elements, as in Figure 2.1, and the axial positioning is locked with rings at the extremities of one bearing.

2.3 Statistics of the normal distribution

Whenever data is analyzed, it is fundamental to characterize it in the form of a statistical curve. Whenever the data shape fits the Gaussian curve, also known as the normal distribution, it is possible to extrapolate meaningful results starting from two values associated with any data set:

- Mean value
- Standard deviation or variance

The mean value μ is obtained by computing the arithmetical average of all the values of the dataset, presented in Equation 2.1.

$$\mu = \sum_{i=1}^n \frac{x_i}{n} \quad (2.1)$$

Where n is the number of elements in the data set, also known as sample size.

The standard deviation σ is a value that represents how spread the values are with respect to the mean value. A higher value of standard deviation implies that there is more variability in the data set, a small value instead means that most of the data set is concentrated around the mean. In the most used formula in the literature, the variance is computed, which is simply the standard deviation squared, as presented in Equation 2.2.

$$\sigma^2 = \sum_{i=1}^n \frac{(x_i - \mu)^2}{n} \quad (2.2)$$

Once the standard deviation and the mean value are known, it is possible to reconstruct the normal distribution that fits the data set. which is done with the Gauss formula shown in Equation 2.3.

$$f(x|\mu, \sigma) = \frac{1}{\sqrt{2\pi\sigma^2}} e^{-\frac{(x-\mu)^2}{2\sigma^2}} \quad (2.3)$$

The curve meaning is strongly linked to the probability of a value to occur [5]. The area between two x values and the curve represents the probability of randomly picking a value between the two x values chosen. In the case of the Gaussian distribution, the graphical representation can be avoided since there is a strong mathematical link between the standard deviation and the probability of occurrence. By choosing a specific amount of standard deviation, generally known as Z , to include in the range, it is possible to directly find the probability from standardized tables, such as Table 2.1.

TABLE 2.1: Probability chart for varous Z values (Most commonly used for statistical analysis in bold)

| Z (-) | Probability range (%) |
|-----------------|---------------------------------|
| 1.04 | 70 |
| 1.28 | 80 |
| 1.645 | 90 |
| 1.96 | 95 |
| 2.58 | 99 |

Equation 2.4 is used to compute the extreme values of the field considered with the respective probability range. I is the interval, X_- and X_+ are the minimum is the maximum value of the field, Z is the value chosen from Table 2.1.

$$I = [X_-, X_+], \quad \text{where } X_- = \mu - Z\sigma \quad \text{and} \quad X_+ = \mu + Z\sigma \quad (2.4)$$

2.4 Temperature measurement theory

2.4.1 PT-100 temperature sensor

The PT-100 sensor is one of the most common Platinum sensor in the industry and belongs to the RTD family (resistance temperature detector). It is used for its reliability and precision of the measurement once the calibration is performed. Some of the most well-known advantages of such technology is the linearity between temperature measured and voltage read on the instrument, as well as the accuracy even at higher temperature ranges. Usually the utilization range varies between -200 to 850 °C [6].

2.4.2 2-Wire and 3-Wire configuration

The 2-wire configuration works on a simple physical property of Platinum. When the material raises its temperature, the resistance of the wire increases. For this reason, by letting a constant current pass through the Platinum wire, it is possible to evaluate which is the voltage across the sensor, hence resistance and consequently the temperature. From this introduction, a simple two wire configuration, shown in Figure 2.2, would be enough.

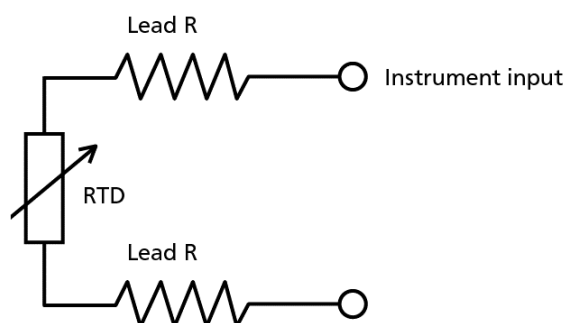


FIGURE 2.2: 2-Wire configuration schematic [7].

The Lead R is the wire connecting the sensor with the PLC module recording the data. Since these wires have their own resistance, the temperature reading must be scaled properly with the calibration. This operation could not be enough if the use of the sensor is extensive and covers a wide range of temperatures. For this reason, the 3-wire PT-100 is implemented.

The instrument has a 3rd wire, shown in Figure 2.3, with very high impedance to allow most of the current passing through the main wires. From this combination it is possible to compute the voltage drop on the lead wire, hence to take it away from the final value logged in the PLC system.

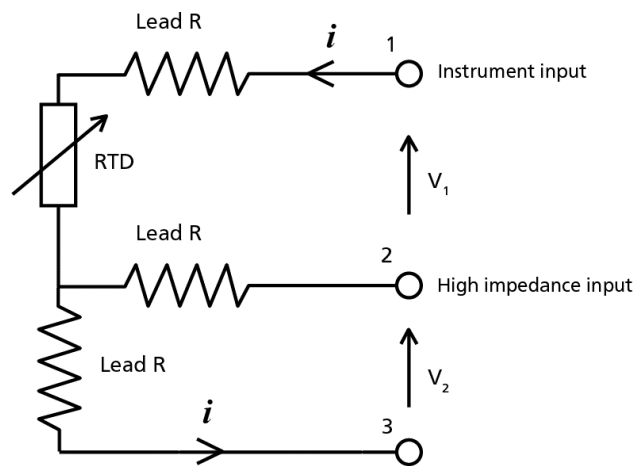


FIGURE 2.3: 3-Wire configuration schematic [7].

There is also a 4-wire configuration, that allows even more precise measurement, but the accuracy requirements of the system are not so extreme, so a 3-wire configuration is chosen.

The resistance value obtained from the PT-100 sensor has still to be translated into real temperature. This is possible by the use of Equation 2.5, from which the actual Equation 2.6 used in the computation is obtained..

$$R = R_0(1 + \alpha(T - T_0)) \quad (2.5)$$

$$T = \frac{1}{\alpha} \left(\frac{R}{R_0} - 1 \right) \quad (2.6)$$

In the above mentioned equations R is the resistance of the PT-100 at the temperature T. α is a constant provided by the manufacturer and depends on the

properties of the material used for the sensor, while R_0 and T_0 are defined as reference temperature and resistance, and correspond for example to 0 °C and 100 Ω .

2.4.3 PT-100 calibration process

The calibration process for the PT-100 is tested or performed with the standard process [8]. The process can be followed with the two simplest measurement points. The one at 0 °C, performed in a mixture of ice and water, and at 100 °C, with boiling water. Before this process, a good solution to test the sensors to have a qualitative idea of the condition, is to tape them all together and to see what kind of reading they have.

Once the data is obtained from the ice bath and the boiling water, there are two possible outcomes of the calibration: either the sensor is calibrated, meaning that its measurement is within the declared accuracy to the measured temperature, or the sensor is not calibrated, so a correction term will be applied to calibrate it.

In general it is possible to assume a linear shift of the reading with respect of the true measurement, so in order to compensate for it, an additive term is inserted in the computation to restore the closeness to the true value. It is important to remember that this is not the only source of error in the measurement. Also the wiring, the system and the user errors play an important role in the measurement final output. Moreover the experiment conditions for the calibration are considered as given, but in reality some errors could come also from that. For example in the boiling water experiment there will be always a gradient inside the water, where small pocets of water could be a little less than 100 °C.

Chapter 3

Research method and equipment

In this chapter, a detailed description of the system and the main problems treated in this thesis are presented and discussed with the possible solution that could be implemented.

3.1 AMB³ test bench working principle and starting setup

The AMB³ is a device designed and entirely realized in the Aalto university, at the Paperikoneet (Paper machine) laboratory. The setup, presented in Figure 3.1, was developed for a previous thesis work to show how practically the backup bearing of a system can be tested.

The machine is composed of several components, which run altogether to monitor, operate and control the system whenever in action. The system may be divided in the following parts:

- Shaft assembly
- Motor and belt engagement assembly
- Holder plate engagement assembly
- Backup bearing support assembly
- Measurement, data acquisition and control system
- Data analysis and MATLAB[®]

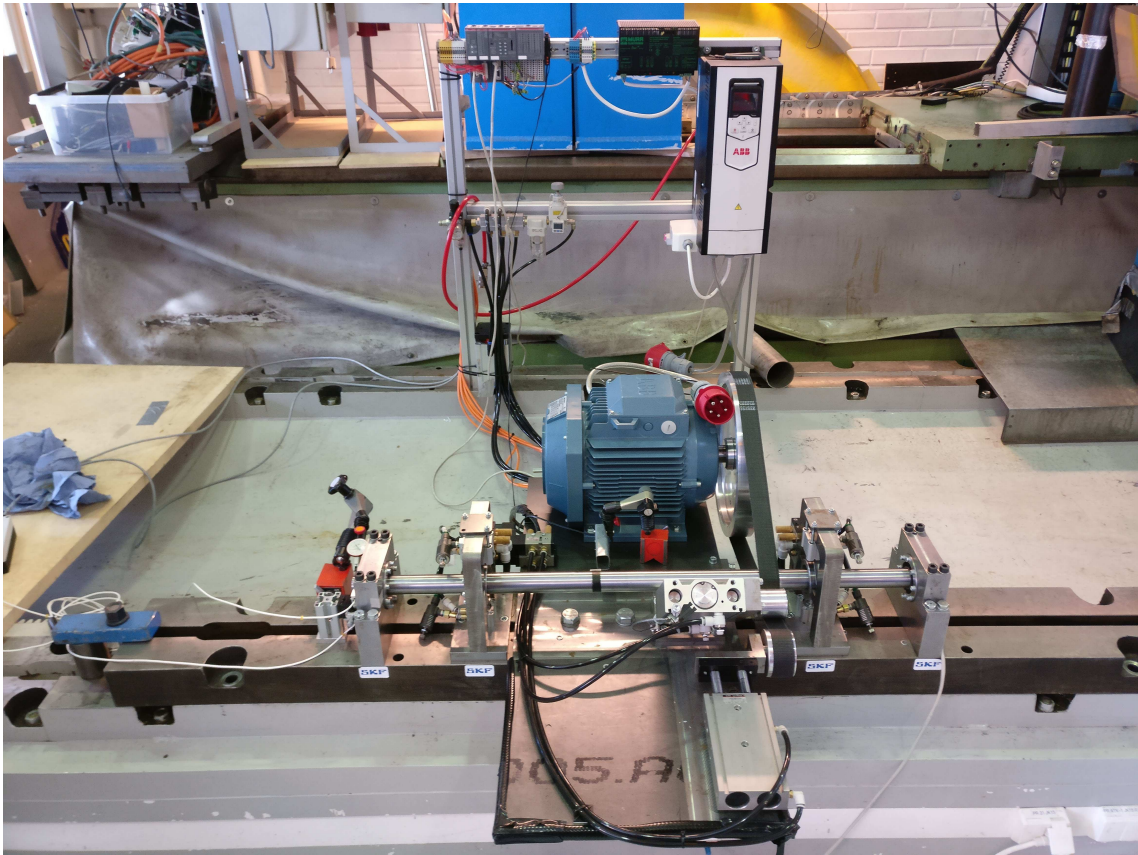


FIGURE 3.1: AMB³ system setup (Aalto university Paperikoneet laboratory)

3.1.1 Shaft Assembly

The shaft assembly is composed of a 1.04 m long spindle, which has 2 shoulders symmetrically placed at approximately 0.2 m from the ends. The smaller diameter is 34.5 mm, while the bigger one is 37.0 mm. It is worth noting that, due to previous usage of the shaft, the tolerances on the ends of the shaft are not tight and some damages are present at the height of the backup bearing position.

The previously mentioned shoulders are present to accommodate the inner ring of the primary bearing. These bearings are the ones that support the shaft while in acceleration. There are two bearings for each side, enclosed in a bearing case that engages with the holder plate system to be held in position or released. The bearings used for this machine are Super-precision bearings from SKF, specifically S7190 CBGA/HCP4A.

3.1.2 Motor and belt engagement assembly

The motor of the system is an ABB motor, presented in Figure 3.2 (right), capable to run up to 3000 rpm. The motor is provided with a 350 mm disk where a simple polyester reinforced rubber belt is accommodated. The belt, which is 1 mm thick and 1.76 m long, runs in between two rollers on a movable support, and then through a final roller that provides the tensioning in the system. Both the positioning and the tensioning is performed by means of pneumatic actuators.

The system was designed so that the tensioning piston exerts a weaker force than the positioning one, so that it will adapt to the engaged and non engaged position of the assembly. The engaging operation consists in the positioning piston sliding down and pressing the belt on the shaft, so that the friction between the belt and the shaft will allow rotation. It is observed that even at high speeds, there is no slip between the belt and the shaft, since the speed ratio between disk and shaft, provided by the data acquisition system, always remains at 9.3. The assembly is shown in Figure 3.2 (left) .



FIGURE 3.2: Belt engaging system (left) and motor assembly (right)
(Aalto university Paperikoneet laboratory)

3.1.3 Holder plate engagement assembly

The most delicate part of the system is the holder plate assembly, shown in Figure 3.3. It is composed of two pneumatic pistons that close and open simultaneously to grab the main bearing cases on the shaft. The locking force is exerted through holder plates, that in the current setup are designed to have a plane to cylinder contact.

The positioning of the shaft center is determined on each support by a couple of screws with a custom end, that constrain the vertical positioning of the holder plate. one of the two screws has a conic end, while the other has a flat head. The conic end inserts into a special conic hole in the upper holder plate, while the other acts as a planar support.

The two pistons, CQ2B32-5DZ and CQ2B40-5DZ with respectively 32 and 40 mm bore diameter, are activated with the same pressure. Due to the difference in diameter, the lower one as a slave and the upper one as a master. The setup pressure is 0,15 MPa, so approximately the two pistons exert a force around 120 and 190 N.

3.1.4 Backup bearing support assembly

The backup bearing assembly, presented in Figure 3.4, is composed of a support that holds the bearing case in position. The support is composed of two parts which are bolted together to hold the bearing case in position. The circular hole in the support was machined with high tolerance levels, and can be used as the reference point for the centering of the shaft in the system.

The bearings used in the backup bearing assembly are produced by SKF, precisely 7007 CDGAV/HCP4A. These are simple ball bearings, and as before they are in couple, held with pretensioning in X configuration. These bearings have an internal diameter of 35 mm, which allows to have approximately 0.25 mm of clearance for the drop down of the shaft.

3.1.5 Measurement, data acquisition and control system

The measurement system, in the initial disposition is equipped with 3 sensors and is controlled by a ABB system that records the data and performs all the controls on the pistons and motor.



FIGURE 3.3: Holder plate assembly in the engaged position (Aalto university Paperikoneet laboratory)

Two sensors are based on the eddy current principle, Figure 3.5 (left). They are used to measure the distance of the shaft, and are positioned perpendicularly to each other, in order to have a X-axis and a Y-axis reading. They are connected to the ABB system by means of an amplifier. The third sensor, Figure 3.5 (right), instead is a Omicron infrared frequency sensor, that points a laser to the shaft, on a half black and half white duct tape. From the frequency of the change of the signal, the shaft rpm are computed by the ABB system.

The logic of the machine is all built by means of ABB Automation Builder program which gathers the data and organizes it in a single ZIP file for the MATLAB[®] script to work on.

The UI is built in the Java[™] environment and allows to control the machine, as well as to see some live parameters recorded by the sensors. It allows to control independently each piston setup, the speed and the on-off condition of the motor, as well as to start the measurement run.

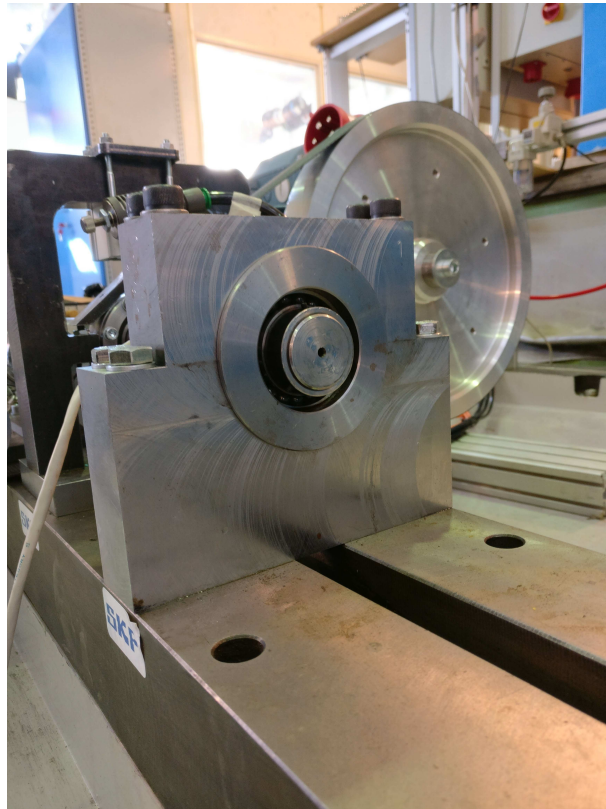


FIGURE 3.4: Backup bearing support assembly (Aalto university Pa-perikoneet laboratory)

3.1.6 Data analysis and MATLAB®

The data acquired by the ABB system is processed by a MATLAB® script that fetches and interprets the data as well as produces visual graphs of the data in time. The code used is presented in Appendix 1.

The first script is a simple bit of code that creates a directory for the data to be stored, with the associated date and time. Secondly it fetches the file *MIT-TAUS.ZIP*, where all the data from the ABB Automation Builder is stored and executes a second script called *Wav_read_ver6.m*, which produces the visual graphs used in the centering process.

The second script presented is responsible for the plot creation. First of all the constant for the transformation from voltage to displacement of the eddy current sensor is declared as *volcalc*. Secondly 3 files are opened where the data from the 3 sensor is stored, and a vector of the required length is allocated. At this point

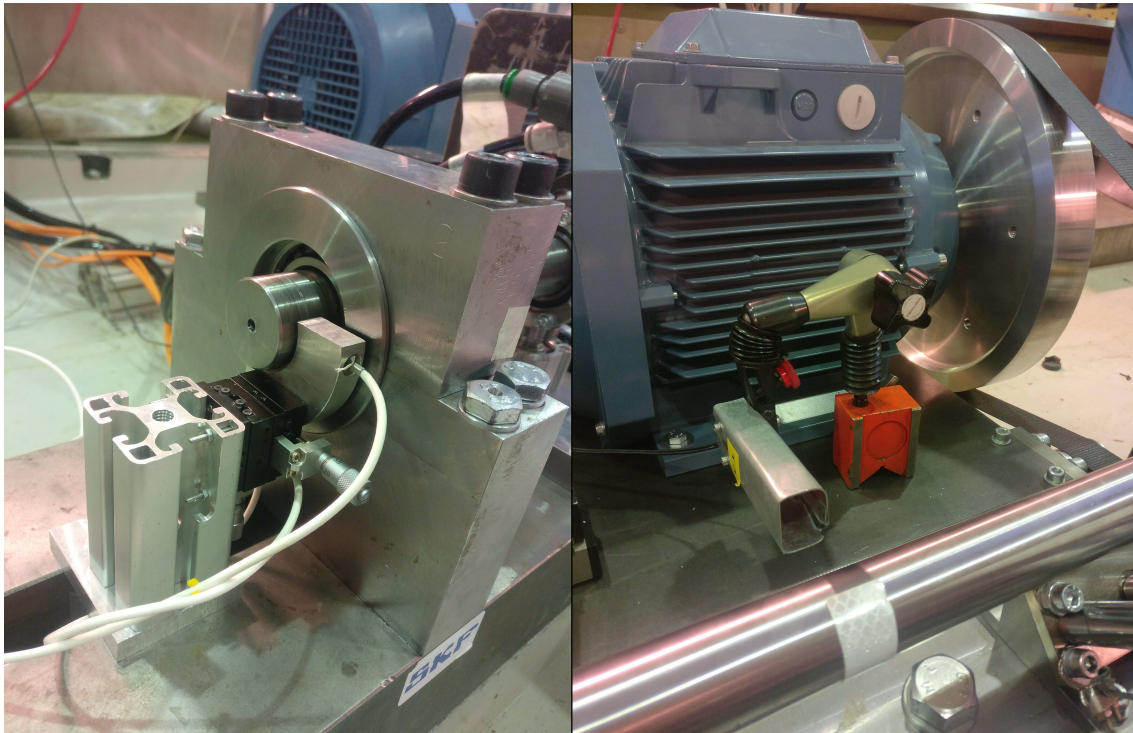


FIGURE 3.5: Measurement sensors: XY positioning Eddy current sensor (left) and frequency sensor (right) (Aalto university Pa-perikoneet laboratory)

the plot the X-Y plot in μm and mm, the X and the Y plots in time domain are created and the figures are saved. For the rpm plot, the speed is computed by a count of the revolutions, and then the figure is created from the data obtained and inserted a figure alone, and together the X and Y plots in time domain. Finally a zoomed version of the X-Y plot is generated and saved.

3.1.7 User interface (UI)

The UI developed for running the system, presented in Figure 3.6, is coded in JavaTM language, and allows to execute some simple actions on the pistons and to execute automatic and manual measurements.

The measurement column contains commands to execute the manual measurement (*Start measurement*), that will give back a reading of speed and position in time as the machine is operating, while the automatic measurement (*Start automatic measurement*) will operate the machine starting from a still position, accelerate it, detach the belt and drop the axle for 2 seconds and then engaging again

the holder plates.

The second column called Maintenance allows to engage and disengage the belt (*Axle detach false/true*) and to apply the belt tensioning (*Detach spring false/true*).

In the Control column, it is possible to set up the speed (*Click here to set speed*), to run the shaft (*Drive start*) and to engage and disengage the holder plates (*Drop axle false/true*).

In the last column, some live measurement are shown, such as speed of the axle, xy positioning from the eddy current sensors, the number of revolutions and the motor rpm.

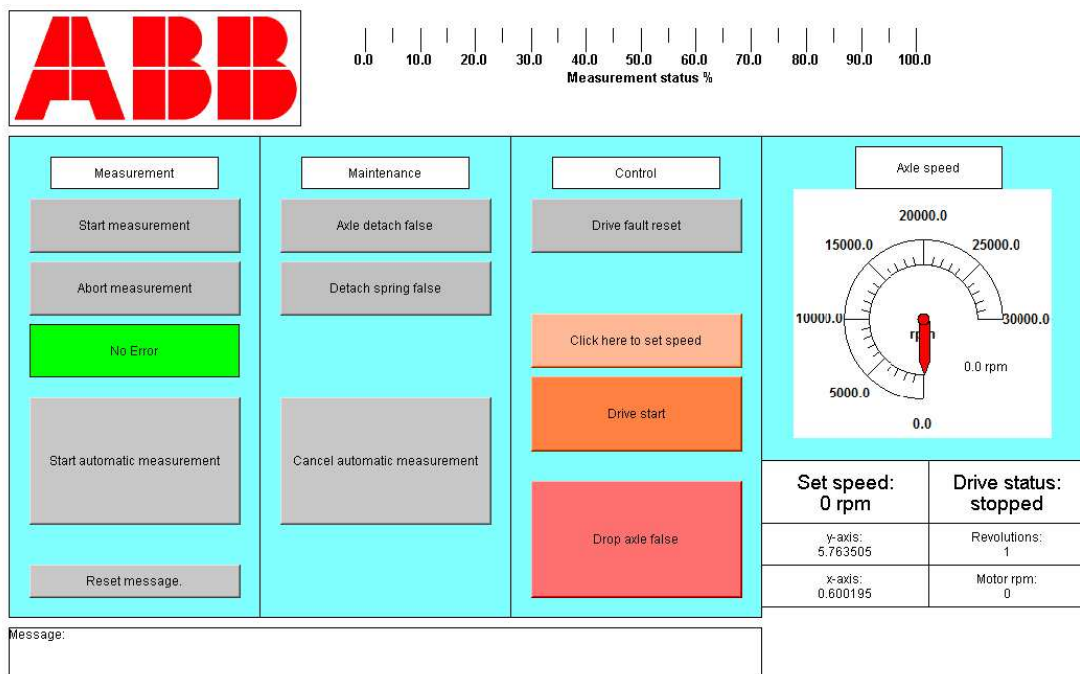


FIGURE 3.6: Java interface to operate the AMB³ test bench

3.1.8 Output of the measurement system

The measurement system data, obtained from the sensors, is fetched by MATLAB[®], which interprets it to output 4 figures. The figures allow to have single graphs related to speed of the shaft and position.

The first chart presented in Figure 3.7 is relative to the XY position of the shaft during the measurement run.

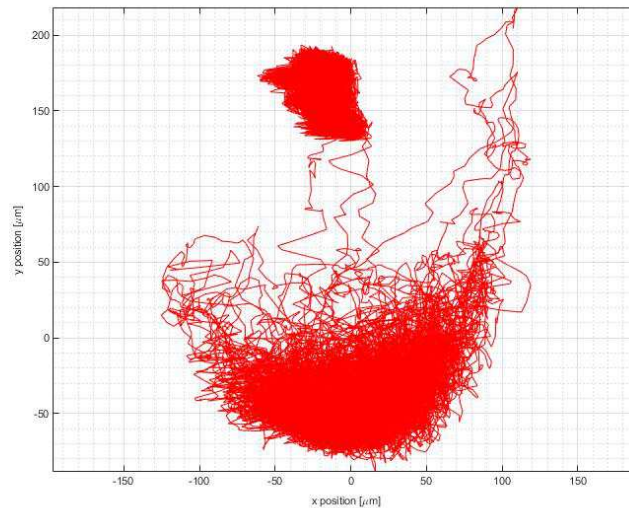


FIGURE 3.7: XY position of the shaft during the measurement run

The second chart, shown in Figure 3.8, shows the speed registered on the shaft by the infrared sensor. The steps present in the plot depend on the way the speed is computed. Since the rpm of the shaft are deduced from the rotation count in a time frame, if the sensor reads one revolution more or one less, there will be a sudden increase or decrease of the speed in the chart.

The third and fourth chart, respectively in Figure 3.9 and 3.10, present a comparison between speed and XY positioning. In the first one it is possible to see again the XY chart scaled both in μm and mm , with the X and Y evolution in time, while in the second the X and Y position in time is compared with the speed.

The measurement system is not only capable of taking the measurement data during the drop down, but also during normal rotation of the shaft. The data obtained in this scenario is particularly useful to evaluate how the centering of the holder plate is, by considering the extremes reached on the X and on the Y axis.

3.2 Setup procedure and calibration of the machine

In the initial condition, the setup of the machine is a straightforward procedure that is composed of simple steps. As a first step, the holder plate pistons must

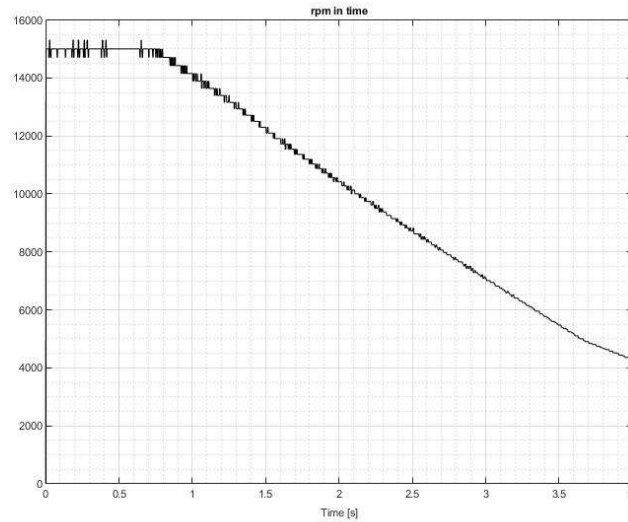


FIGURE 3.8: Speed of the shaft during the drop down

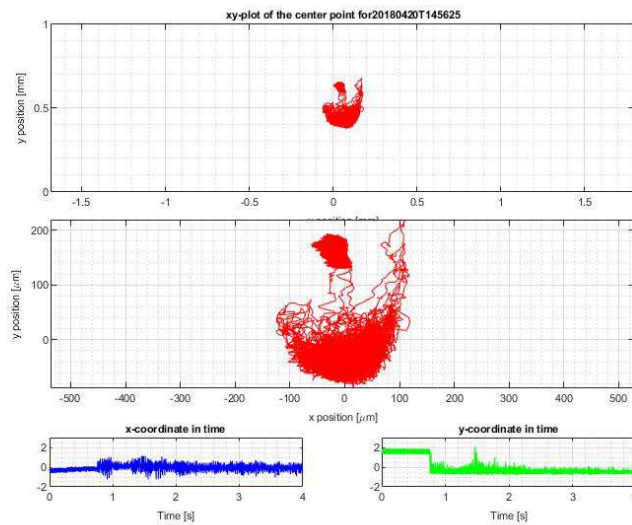


FIGURE 3.9: XY positioning and single axis evolution in time

be in the disengage position, in order to let the shaft and the bearing cases slide inside the holder plates. It must be remembered that also the belt tensioning and engaging system must be disengaged to allow the shaft to be positioned.

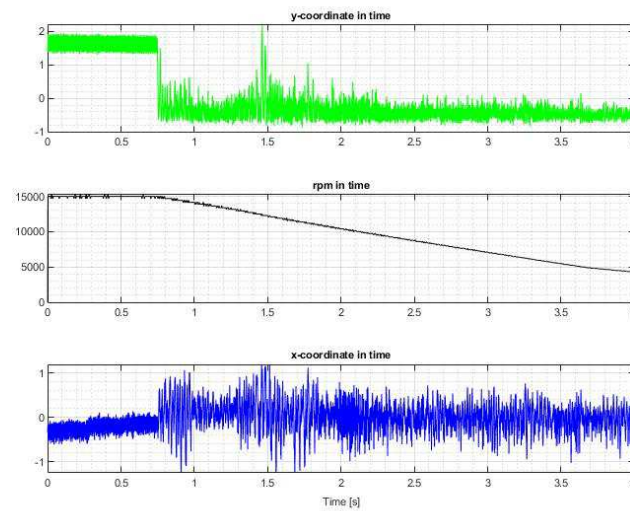


FIGURE 3.10: X and Y evolution in time compared with the shaft speed

With the holder plates disengaged, it is possible to fit the shaft inside the supports. At this moment the backup bearing case are still to be positioned, but the backup bearing support are already tightened, since they will be used as a reference point for the shaft centering. It is possible to use the internal circumference of the support because it was machined with a high degree of precision. The shaft and the primary bearings cases are slightly larger than necessary, so the axial position can vary in the range of approximately a centimeter without affecting the performance of the system.

At this point the holder plate pistons are engaged to lock the shaft in a first tentative position, and it is possible to measure the distance of the shaft from the backup bearing support. The distance measurement is performed with a Tekusa Type Mu indicator stand, which has a magnetic connection which makes it able to couple to the shaft and rotate with it. Every time some modification of the holder plate position has to be done, the pistons must be disengaged, the screws must be moved accordingly to the modification required, and then the piston can be engaged again. The vertical centering is performed only by the screw position, while the horizontal one can be a combined action of the movement of the support, and the motion of the screws. It must be remembered that the positioning of the backup bearing supports has to be perfectly square to the frame of the machine, otherwise the backup bearings will not have the necessary clearance to work.

Once a satisfying position of the shaft is reached, the support can be opened to insert the backup bearing case in its final position. Once the support is tightened, the shaft should be able to rotate without any movement of the backup bearings. A first test can be done by engaging the belt and letting the shaft rotate up to 10000 rpm. It is possible to hear that in this range the system is moving through its resonance frequency, and for some moments the vibrations are intense. If the backup bearings do not move during this phase, the calibration of the system can be considered successfully.

3.3 Issues with the initial setup

Even if the system is properly calibrated with the previously explained procedure, some problems arise with the continuous use of the device. First of all, the maximum speed for which the system was designed is 28000 rpm for the shaft. At this speed the holder plates have not enough strong clamping force to keep the shaft stable with low vibrations.

A second problem that becomes more evident with prolonged use of the system is that, during the acceleration to high speeds, the system passes two of the natural frequencies of the shaft. The induced strong vibrations of the whole support system let the screws to lose the position set in the calibration procedure. As it is possible to see, after some tests, the shaft lowers its positioning, and rests on the backup bearings even if the holder plate pistons are still engaged. This behavior requires a new calibration procedure which affects the usability of the machine.

While the measurement system is working flawlessly in the initial setup, it lacks more depth to the parameters measured. An addition of some temperature measurements and more graphs would be extremely helpful to better characterize the behavior of the backup bearings. This addition would be also useful for a computer model project developed at the Lappeenranta University of Technology.

3.3.1 Holder plates design

The initial setup upper holder plate locks with a 40° angle the bearing case in two points. While there is no problem with the upper one, the lower one, presented in Figure 3.11 was designed to support the primary bearing case on a planar surface. The design was not perfect since in the end the bearing case rested not on the lower holder plate itself, but on the bolt locking it to the piston. The surface of the screw was not machined to accommodate smoothly a cylinder to plane contact, so it was modified on a lathe. Some material on the bolt head was removed in

order to let the cylinder rest on the actual machined surface of the lower holder plate. No further modification is required since the contact area that previously was on the bolt flat head corresponds approximately to the contact area on the holder plate ring.

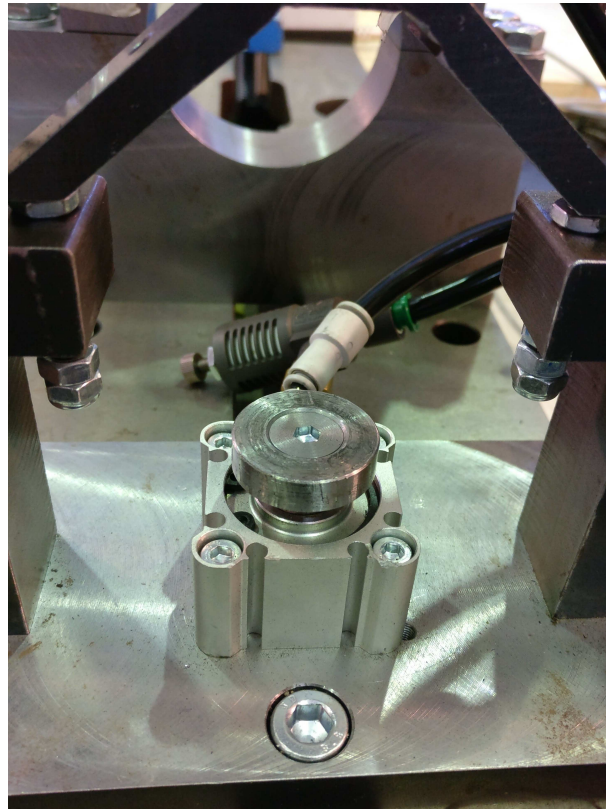


FIGURE 3.11: (Aalto university Paperikoneet laboratory)

3.3.2 Screw design

The screws used for the upper holder plates positioning are standard threaded M6 screws. They are inserted in a threaded hole which keeps them in position, but there is no possibility of locking them during operation. This leads to the loss of positioning during operation, due to the strong vibration of the shaft and the motor.

3.3.3 Damaged backup bearings

On the right side of the machine, the backup bearings are not properly working. Upon inspection it is clear that they do not roll properly. Most likely this is due to some dirt that managed to get into the bearings and damage some of the spheres inside. Moreover the damage is made more clear from the fact that there is some oil spillage from the internal parts of the bearings to the outside.

This hypothesis comes from the fact that, during use, it was noticeable that some sparks would form when the inner ring of the bearing was briefly in contact with the locking ring of the shaft. This situation occurs during the drop down test, when the shaft is not axially constrained unless the locking rings touch the bearing inner ring. It can easily happen that the sparks, which are small particles of steel, fall into the bearing, and upon continuous use, they can accumulate up to the point where there is enough material to damage the bearing.

It would be beneficial for the setup to have some plastic caps to cover the bearings, but since this problem was noticed later during the work, a simple substitution of the damaged bearings will be done.

3.4 Temperature measurement introduction

The temperature measurement is set up in order to obtain the temperature data on the outer ring of the backup bearing, the temperature of the backup bearing support, and the ambient temperature related to time and to the speed of the shaft. The temperature set up is done with the implementation of a NI system.

The measurement of ambient temperature and the support one is performed with a single measurement. To have a more precise profile on bearing temperature, a 4-point measurement is set in 4 cardinal position, defined as up, down, left and right. This is necessary since the shaft mainly has contact with the lower part of the inner ring at lower speeds, so it is interesting to know if there is a more marked heat transfer to the lower part instead of the higher one.

In order to have more usable data for further projects, such as the AMB³ test bench computer model, instead of only graphical representation of the temperature behavior, also a data log of the temperature in time domain. The coupling with the shaft speed is simply done by tracking the time of start of the measurement run and the time of the drop down. Then from the speed data from the ABBs it is possible to plot together all the charts.

Regarding the ambient temperature, it is preferred to consider two different point of measurement. This is due to the fact that the machine is enclosed in a safety cover that should block any projectile in case of malfunction. Due to the cooling apparatus of the motor and the rapid rotation of the shaft, the internal part of the enclosure is subject to a noticeable flux of air. This could lead to unreliable data on the ambient temperature, so an auxiliary temperature outside the enclosure is useful to see if there is any bias.

Chapter 4

Results

In this chapter the main analytical results are presented, with some graphical representation of the data.

4.1 Vibration analysis

The vibration analysis is performed to have a qualitative evaluation of the resonance values of the system. It should be considered as a remark of which speed are to be avoided when using the system. It is difficult to perform it analytically since there are more than one rotating masses, with different angular speeds, so the practical data drive approach is used.

The evaluation is done by means of the accelerometer of a smartphone, precisely the OnePlus 3T, which has a satisfactory level of accuracy for the purpose of the study. The sensor is placed on the plate, and 10 s of vibration at each speed are recorded. Once the data is acquired, it is transferred in Microsoft Excel, and studied. Considering a normal distribution for the data acquired, with a 99 % confidence level, the maximum and minimum amplitude are taken, and a plot is made with all the data for each speed.

The speed partitioning is done every 100 rpm considering the motor speed. All the data collected is presented in graphical form in the Appendix 2.

The results of this analysis, reported in Figure 4.1, denote the main resonance frequency around 1100 rpm for the motor (equivalently 10230 rpm for the shaft), where the vibration become increasingly big. It is noticeable during operation, that if the critical speed is not passed quickly, the vibration of the system induces

the shaft to touch the backup bearings and make them rotate. As soon as the resonance point is passed, the contact ceases.

Regarding higher frequencies, there is a second resonance point at 1500 rpm (13950 rpm for the shaft), where some mild vibration are perceived, but no contact happens between the backup bearings and the shaft. A third resonance point from the data seems around 2800 rpm (26040 rpm for the shaft), but in this high speed range the validity of the measurement can be questioned, due to the sample rate of the accelerometer fixed to 200 S/s. This is due to the fact that it is a common rule in the measurement field to have at least an order of magnitude between the frequency of a phenomena and the sample frequency, for a perfect measurement.

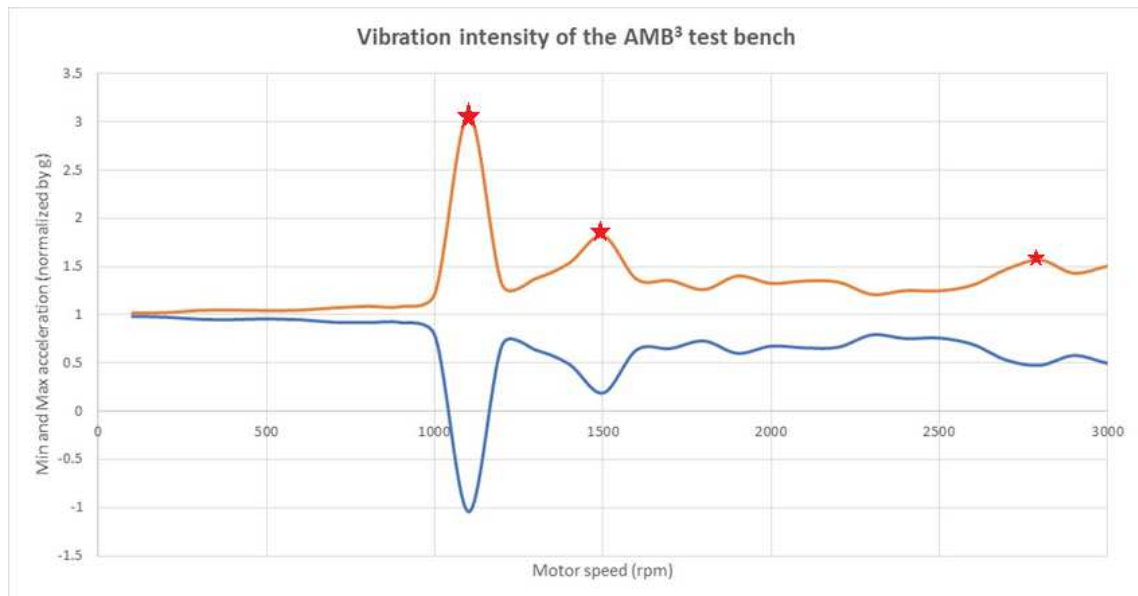


FIGURE 4.1: Results of the vibration evaluation with 99 % confidence level

On a deeper inspection, as presented in Figure ??, excluding the shaft from the analysis of the vibration and letting the motor spin free, it is noticeable that the motor itself is the cause of the vibration in at 1500 rpm. Toward higher frequencies, over 2500 rpm, the vibration becomes constant, most likely because the motor is exiting his standard design condition, and so it starts to have some problems containing the vibrations. Again, the higher speed values are to be taken with caution, since the frequency is approximately one fourth of the sampling rate, hence could have some unnoticed behavior.

4.2 Shaft centering analysis

The shaft centering analysis is based on the comparison of the center position with and without the nuts holding the positioning screws. The aim of this experiment is to show how the decay of positioning advances after each experiment.

First of all, the system is calibrated in order not to have contact with the backup bearings, and to have a range of vibration at medium speed that is acceptable, so around 60-70 μm . Then a first test run is done at maximum speed to check whether the calibration is properly done. At this point the measurement can be initiated since the machine is in the normal operation condition .

Each measurement run consists in 2 phases. The first one is the acceleration of the shaft up to 15000 rpm and let run for 10 seconds in order to stabilize the speed. At this moment, a measurement of the shaft vibration is taken. The second phase consists in the drop down of the shaft, with the subsequent deceleration. At this point the data is evaluated and recorded. The system is reset by engaging and disengaging the holder plates multiple times, in order to let the shaft reposition itself. Some gentle taps with a hammer could be needed in order to avoid contact between the locking ring and the backup bearing inner ring. At this point the operation is repeated until the data shows that the initial positioning is considered lost.

The results are presented in both in graphical charts and in a tabular form. Most of the graphs are collected in the Appendix 3, in order to keep the section more fluent and to better organize the data.

4.2.1 Centering test without the locking nuts

The system is tested without the locking nuts positioned on the screws. The full device is properly calibrated in order to reach stability at normal speed. Once this condition is reached, the shaft is accelerated to low speeds, around 500 rpm, in order to avoid the first resonance frequency, to let the primary bearings get to the working temperature. Once the shaft has been rotating for a sufficient amount of minutes and no problems are detected with operation, the centering test is performed.

The centering test consists in letting the shaft rotate around 15000 rpm, so a bit higher than the 50 % of its maximum speed, and far from the second resonance frequency of the system. At this point a first measurement is done without the

drop down to see how the centering of the shaft is working. The data obtained from the process is collected in Figure 4.2.

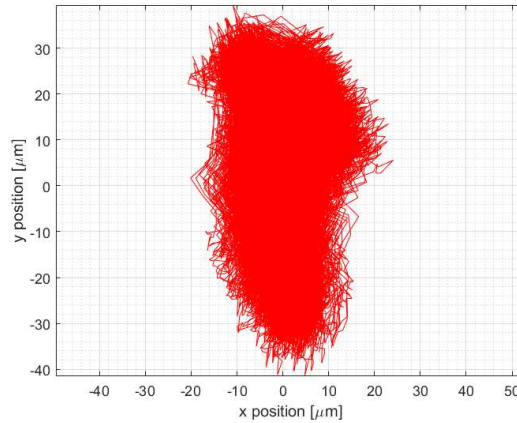


FIGURE 4.2: Centering test performed at 15000 rpm without the locking screws

The data shows already a high displacement of the shaft in the vertical direction, around almost $80 \mu\text{m}$. The horizontal direction is considered stable enough, with a variability of $40 \mu\text{m}$. This condition of high variability on the y axis is not perfect, but not strictly harmful for the system. At this point the shaft is decelerated to start the 28000 rpm test, since no contact occurred with the backup bearings.

Already during operation it is clear that the screw positioning is not holding up as it should. The shaft starts to touch the backup bearings around 22000 rpm, and hardly can accelerate over 26000 rpm. It is possible to see the screws slowly turning due to vibration, and due to some sparks coming from the right backup bearing set, the test is canceled and the machine is decelerated. A new centering test at 15000 rpm, as presented in Figure 4.3, reveals that the positioning is completely lost and the machine is not capable of performing anymore.

As it is possible to see the vertical displacement has increased to $120 \mu\text{m}$, while the horizontal one is around $80 \mu\text{m}$. The system is completely incapable of working after a single attempt to run the drop down, with high risks for the instrumentation and the backup bearings, since there is a 50 % increase on the positioning on the y axis of the shaft.

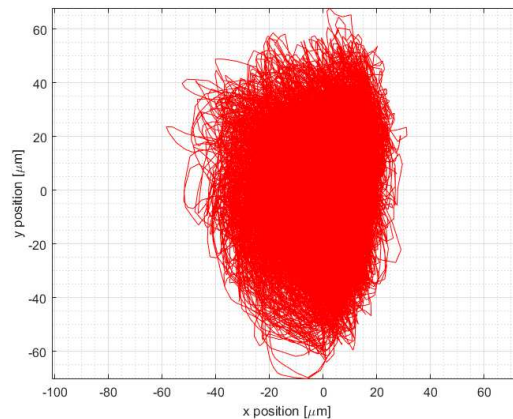


FIGURE 4.3: Centering test performed at 15000 rpm after the failed drop down test

4.2.2 Locking system for the screws

The screws controlling the positioning of the holder plates are simply kept in position by the pressure exerted by the holder plate. This condition is not beneficial for the system, that, as explained before, suffers from strong vibrations at high speeds. Due to the lack of constraint, it is visible that the screws tend to rotate and lower their position during operation, thus making the system at danger of failure. The simple solution equipped in this scenario is to add a couple of tightening nuts that will induce the friction between with the threads of the screws, in order to keep it still for prolonged times.

The nuts, highlighted in red, are positioned both over and under the threaded hole as in Figure 4.4, in order to avoid extreme tightening on one side. If the required torque to lock the screws were to be applied only to one side, it would lead to the loss of the positioning, due to the movement of the screw during the tightening operation. The two nuts are to be tightened at the same time in order to keep the positioning as precise as possible.

Even if this solution is simple, it is nonetheless effective in keeping the positioning screws locked in. The two nuts at the bottom of the screw were added since the screw itself was modified on the lathe, in order to accommodate the wrench for the tightening. They are locked together to offer a point on which apply torque to raise or lower the screws.



FIGURE 4.4: Detail of the positioning of the locking nuts on the positioning screws

4.2.3 Centering test with the locking nuts

The method applied for the previous scenario with the lack of the locking nuts is repeated for the modified case. First of all the system is again properly centered and the 15000 rpm test is performed. The results, showed in Figure 4.5, already shows a much better centering capability of the shaft with respect to the previous case in Figure 4.2, with a horizontal displacement around $55 \mu\text{m}$ and a vertical one around $60 \mu\text{m}$.

Since no problems show up during this process, the shaft is set to rest and then accelerated to the maximum speed of 28000 rpm, and the drop down occurs. It is noticeable that this time, when the shaft is caught again by the holder plates, it spins freely of the backup bearings, and looks perfectly ready to have another run of the test. The results of the analysis is shown in Figure 4.6.

Once the shaft reaches a full stop and the motor is at rest, the belt assembly and the holder plates are disengaged in order to allow the axial repositioning of the shaft. At this point the centering test is repeated, with the results shown in 4.7. In the figure it is clear that the shaft is still centered even if there is a slight increase to $70 \mu\text{m}$ in the X-axis movement of the shaft during rotation, while the Y-axis settles to $70 \mu\text{m}$. This is to be expected since the system undergoes strong vibration and a violent drop down, so with repetition the centering will be looser and looser.

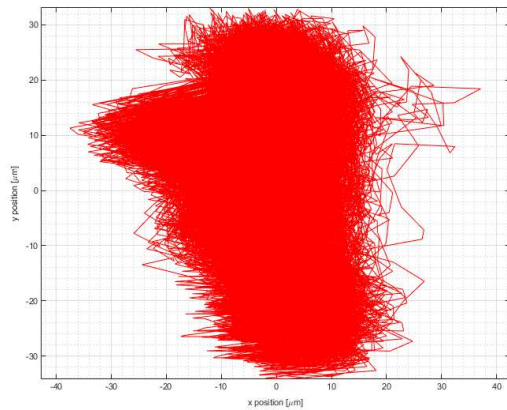


FIGURE 4.5: First centering test performed at 15000 rpm with the locking screws

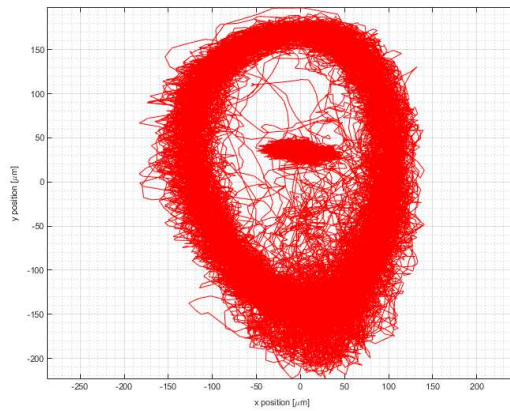


FIGURE 4.6: First drop down test at 28000 rpm with the locking screws

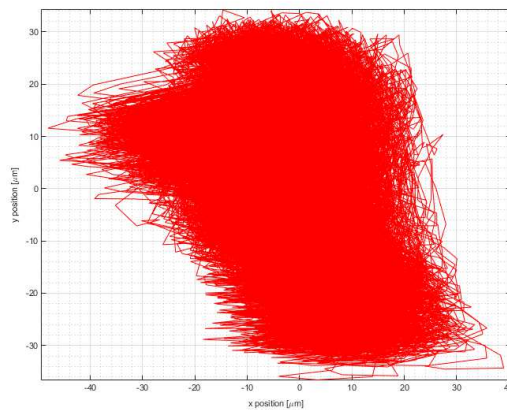


FIGURE 4.7: Second centering test performed at 15000 rpm with the locking screws (Aalto university Paperikonnet laboratory)

The process of drop down, axial repositioning and centering test is repeated several times, and in each test the data is recorded and shown from the summary of Figure 4.8. A more detailed version of the data acquired is presented in the Appendix 3, with all the graphs presented by the MATLAB[®] script in each case.

The process is interrupted at the test n^o 6, since the shaft vibration and the repeated test does not seem to affect the centering, which increases and decreases between each test.

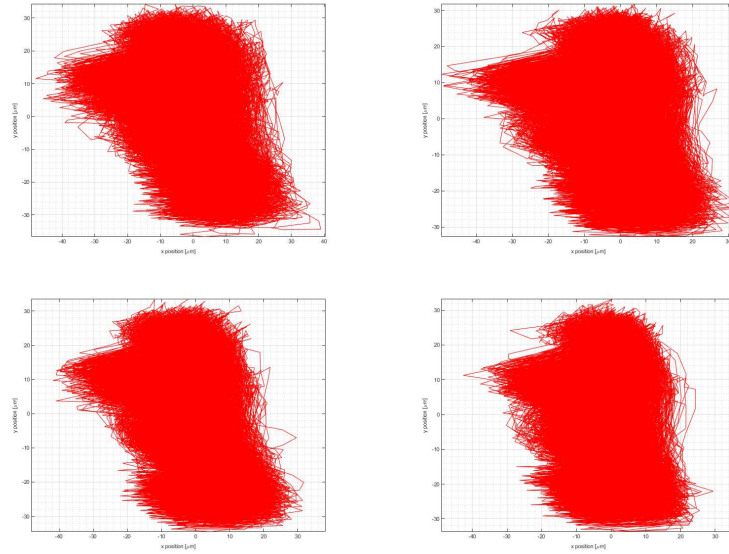


FIGURE 4.8: Centering test 2, 3, 4 and 5 with locking nuts

4.3 Backup bearing substitution

The substitution of the backup bearing is performed in order to guarantee the best condition of the machine. In the initial setup both sides, especially the right one, were not running as smoothly as they should.

The bearing outer ring does not fit the case at ambient temperature, since there is a slight interference between the two cylinder. To insert it in the bearing case, the thermal properties of steel are used. The bearing case is heated to high temperature, in the order of $200\text{ }^{\circ}\text{C}$, while the bearings are cooled to approximately $-10\text{ }^{\circ}\text{C}$. In this condition the two bearings can be pressed inside the bearing case and positioned in the end of it.

At this point the closing ring, which is precisely sized, is bolted to the bearing case. The closing ring applies pressure on the outer ring of one side while a rim on the bearing case applies pressure on the outer ring of the other bearing. A thin disk is placed between the two inner rings and allows to apply the pretensioning on the bearing by locking it in the X configuration.

4.4 Temperature evaluation

The temperature measurement system is developed using the NI software LabView[®]. The software allows to connect the hardware and to move, interpret, process and store the data from the sensors by the use of its interface. It also allows to create a sort of control panel to operate the measurement, to display flow data and to check the status of the system.

4.4.1 LabView[®] and NI system

For the required measurement 7 PT-100 resistors are used from NI, specifically the product 745691 with length of the wire of 2 m. These sensors are produced ready-to-use and have the standard 100 Ω resistance. They are produced following the DIN 43760-1980 standard, today replaced by IEC 60751:2008 [8], and which certifies them to have a declared accuracy presented in Equation 4.1. In the equation, t is the temperature of the measurement in $^{\circ}\text{C}$, while A is the accuracy.

$$A = 0.3 + 0.005|t| \quad (4.1)$$

The sensors are connected to 2 modules NI 9219, design for multipurpose measurement. These modules are connected to a NI cDAQ 9174, which allows to transfer the data to a PC and to communicate to LabView[®]. The NI system is presented in Figure 4.9.

The LabView[®] program developed for the system has two main tasks. The first is to show the data through a chart that updates in real time and lets the user see what are the temperatures on the machine, as well as to have some indicators if the temperature is growing with respect to the ambient one. The second and most important task is to create a file with the data log in time of all the temperatures measured, in order to allow post processing and further study of the thermal behavior of the bearings. The interface used to operate the measurement is presented in Figure 4.10, and shows the chart as well as some light that pop on and off depending on the relative temperature with respect to the environment. There are also buttons to set up the frequency and the samples to be taken at each iteration. It is possible to start and stop the data recording, as well as change the directory and the name of the .xls file with the data log. The program itself from which the interface is generated is presented instead in Figure 4.11, where it is possible to see how the data flows and is processed.

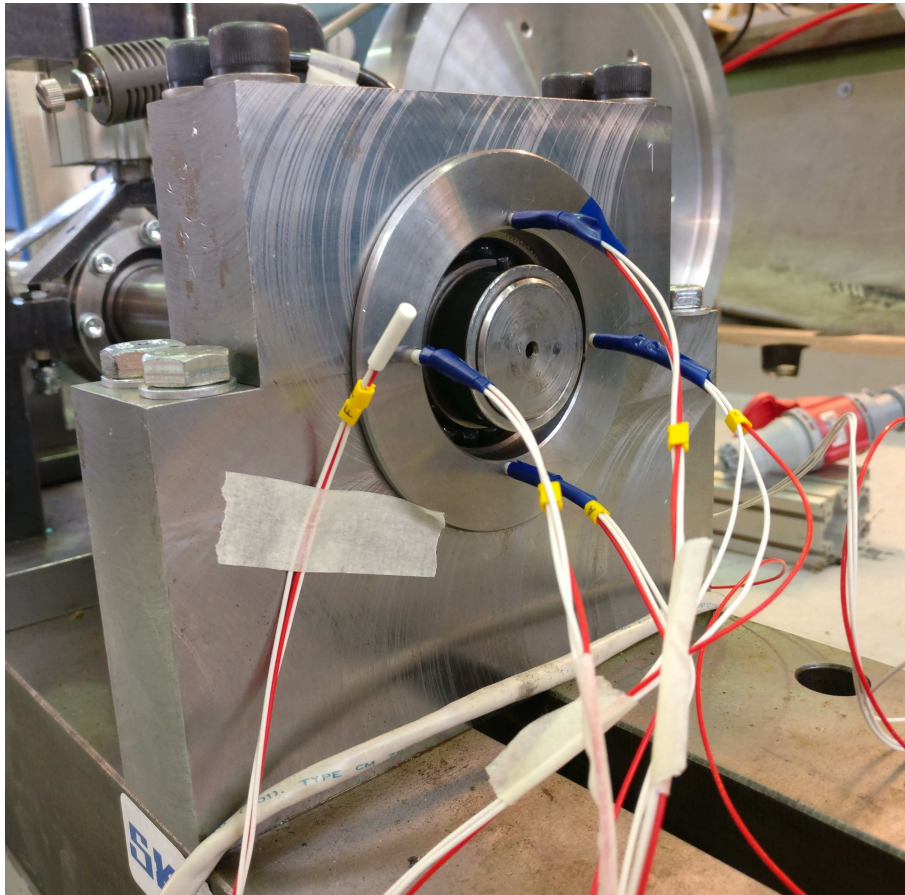


FIGURE 4.9: Measurement setup with the NI system

It is worth noting the signal processing that happens to convert the resistance measured into temperature, shown in Figure 4.12, is the code version of the Equation 2.6 previously presented.

The code is also capable of computing the accuracy of each single temperature measurement, using the Equation 4.1 previously presented. The accuracy is also logged in the final .xls file for further analysis.

The 7 sensors are placed on the system and are coded with a simple scheme that assigns to each PT-100 a letter that is also reported on the cable. This allows for easy management of the cables and quick installation. The cables are named in the VI with the following scheme:

- A_lower : Lower temperature of the bearing
- B_left : Left temperature of the bearing

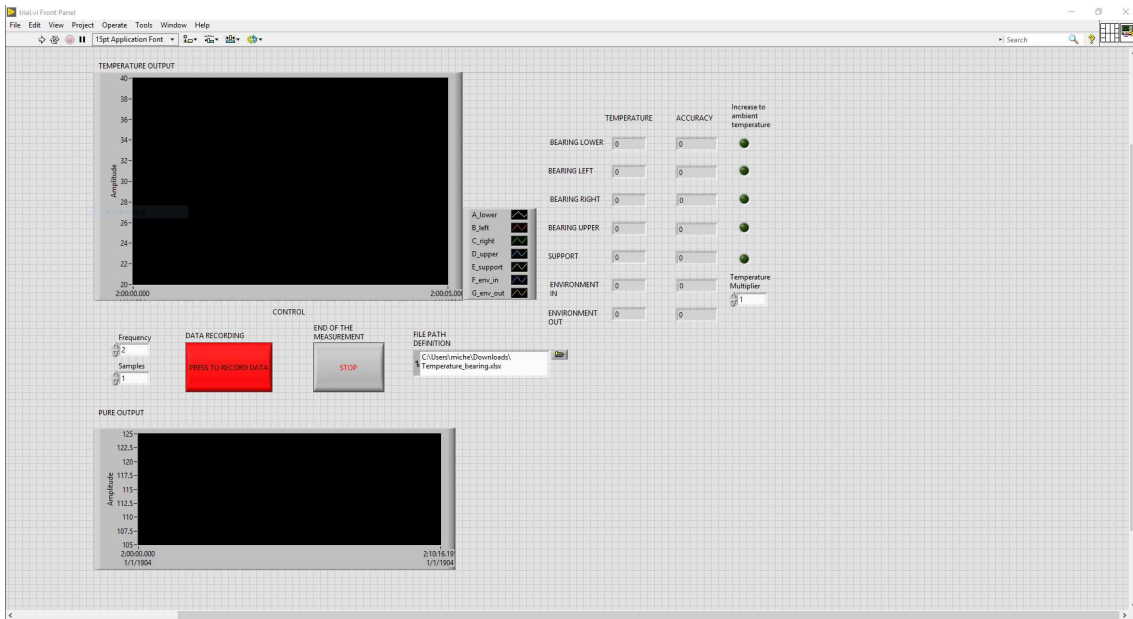


FIGURE 4.10: LabView[®] interface to operate the measurement system

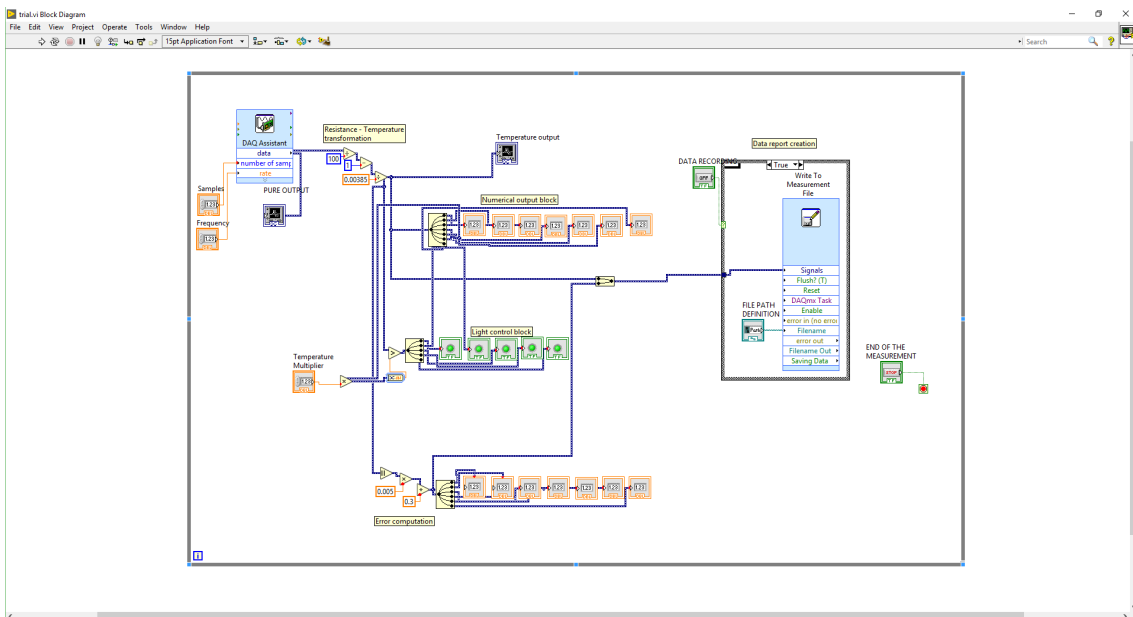


FIGURE 4.11: LabView[®] program which controls the sensor operation

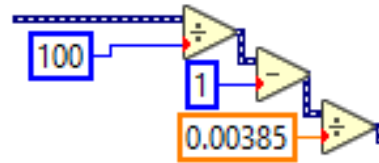


FIGURE 4.12: Detail of the resistance-temperature conversion in LabView[®] code

- C_{right} : Right temperature of the bearing
- D_{upper} : Upper temperature of the bearing
- E_{support} : Temperature of the support
- F_{env_in} : Temperature of the environment inside the protective glass
- G_{env_out} : Temperature of the environment outside the protective glass

4.4.2 Sensor placement

The sensors are placed onto the bearing in order to be in contact with the outer ring in the four cardinal points. To allow this, four 3,5 mm holes are drilled, in order to accommodate the 3,45 mm diameter cap of the PT-100 sensor. The hole itself is enough to hold the sensor in place, but a small quantity of thread seal tape (PTFE) is used to generate some friction that grips the sensor head to the hole walls. More complex system of installation were not considered since they would cause a slow down in the installation operation. Moreover the tape allows to create an insulation between the bearing case and the environment.

On the other hand, the three remaining sensors are placed differently. The support sensor is placed approximately 2 mm from the backup bearing case in order to obtain the temperature as close as possible to the bearings. In this case the hole is much deeper and allows the full insertion of the PT-100 inside. Some attention must be payed in order to avoid the detachment of the cap from the sensor itself. The remaining environment temperature sensors are placed freely in the machine. The internal one is approximately 2 cm far from the bearing, close to the support, while the external one is close to the protective glass far from the machine.

TABLE 4.1: Results of the calibration test

| Sensor (-) | Temperature (°C) | Δ (°C) |
|---------------|---------------------|------------------|
| A_lower | 99.6 | -0.4 |
| B_left | 100.1 | +0.1 |
| C_right | 99.4 | -0.6 |
| D_upper | 99.6 | -0.4 |
| E_support | 99.5 | -0.5 |
| F_env_in | 100.2 | +0.2 |
| G_env_out | 99.8 | -0.2 |

The body of the NI system is placed near the machine and connected via USB to the computer that controls the VI.

4.4.3 Calibration

The calibration of the PT-100 is guaranteed by the manufacturer NI, which sells them in the "ready made" form. This means that the sensors should be perfectly calibrated to be used on the field. However, testing the 100 °C temperature with boiling water is a simple experiment that allows to check if the calibration is properly done. The expected result is to have all the sensor measurement reach the 100 °C for some seconds during immersion. The results of the analysis are satisfactory since all the sensors are within the error range of 0.8 °C from the target temperature. The results are presented in Table 4.1.

The data shows a little bias toward lowering the temperature measured, but it should be not cause of alarm. This kind of calibration tries to measure 100 °C, which is a threshold that is imposed by the nature of water. In reality when we are measuring it is more likely that the temperature will be slightly smaller than the 100 °C nominal value. Moreover the temperature measured in the system are low so there will be a small effect on the final output.

4.4.4 Measurement results

First of all a full temperature measurement is done on a simple drop down test at 28000 rpm. The measurement goes for a long time after the shaft reaches a rest position, since the thermal flow in the steel of the support from the bearing requires a bigger order of magnitude of time. In Figure 4.13 the measurement

in time domain is presented. The frequency chosen for this kind of inspection is 2 measurements per second, since the thermal gradient is not so strong and the flow of heat not so fast.

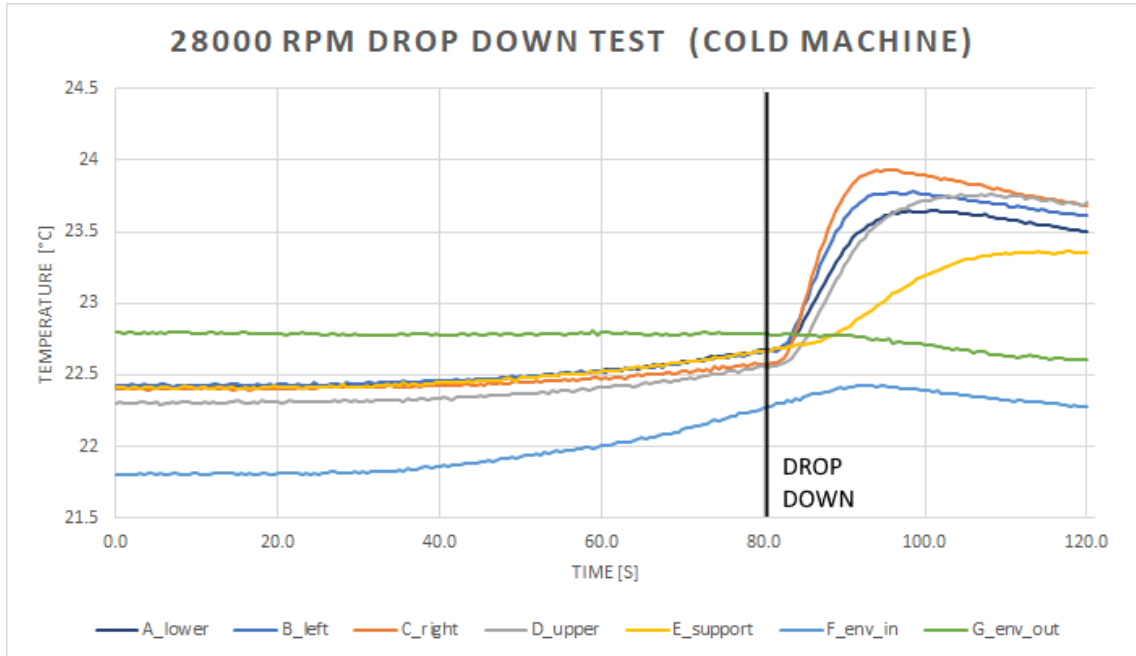


FIGURE 4.13: Temperature of the 7 points measured during a full drop down test from a cold machine

With the VI created, it is possible to extrapolate interesting temperature data with a good timing. In the experiment on the temperature measurement, three different moments were considered interesting for the analysis. A first moment is the preheating phase, where due to the wind generated by the motor it is possible to see the sensors reach a different value with respect to the environment one, a second when the drop down phase happens, and a third one where the heat flows from the bearing inner ring to the outer ring and to the support.

The full measurement run, during an approximately 11 minutes of rotor running to perform the test, shows a stable heating phase for half of the time. The behavior is shown in Figure 4.14.

Considering only the heating part, from the beginning to 340 seconds is presented in Figure 4.15. The heating proceeds constantly for the whole experiment, and it shows the importance of having two separate temperature measurements of the environment.

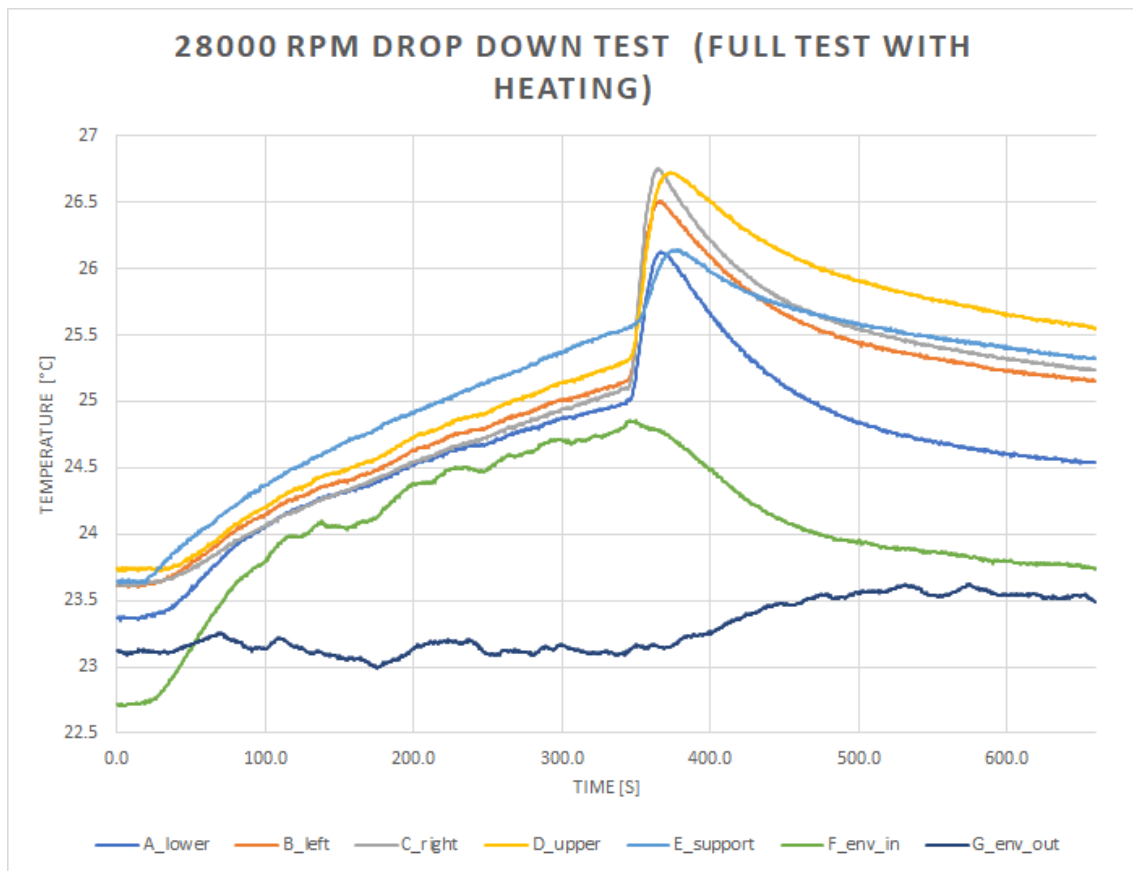


FIGURE 4.14: Temperature evolution during the heating phase

In the last part of the measurement run, from 340 s to the end of the test, the shaft drops down and the thermal behavior of the bearing shows a peak with a small delay with respect to the contact. Figure 4.16 shows the peaking and then a part of the slow cooling action of the environment temperature on the support and on the bearings.

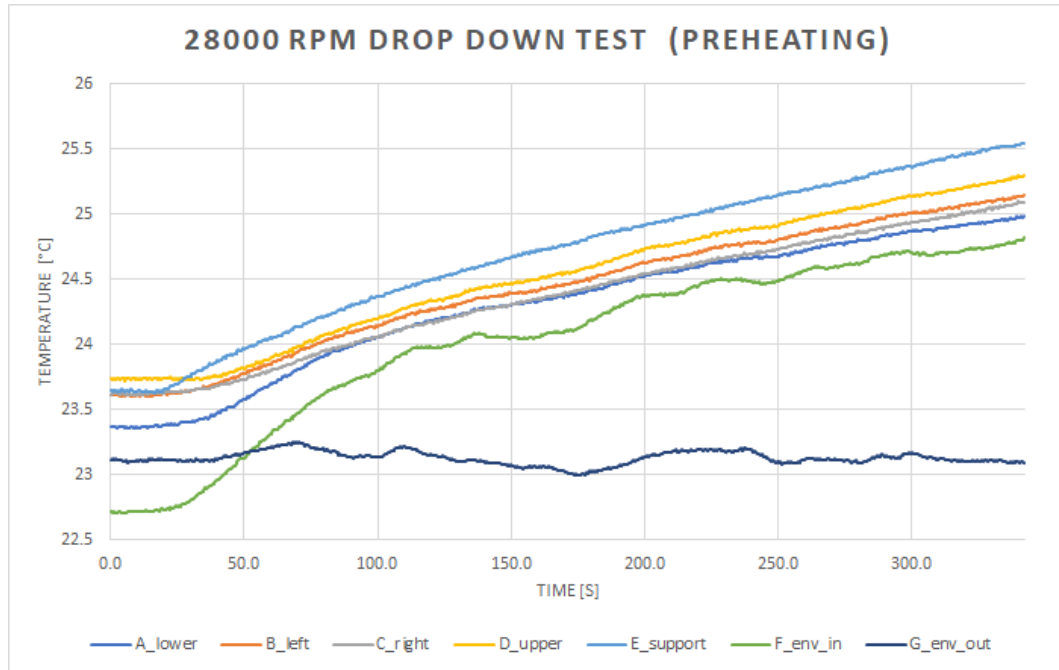


FIGURE 4.15: Temperature evolution during the heating phase

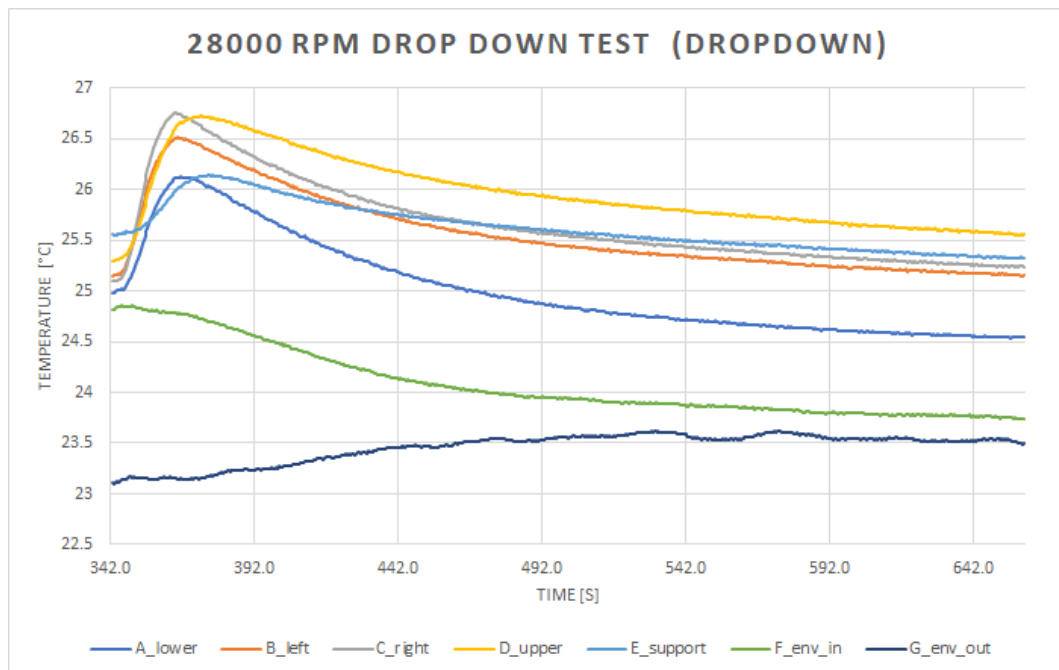


FIGURE 4.16: Temperature evolution during the drop down and cooling phase

Chapter 5

Discussion and findings

In this chapter the results previously obtained are analyzed and some explanation are presented.

5.1 Centering behavior of the test bench

The centering of the shaft during rotation is one of the crucial topics of this thesis. The centering values of X and Y axis are reported in tabular form in Table 5.1 and in graphical form in Figure 5.1. The values do not show the expected centering loss as the test go through, as it happened in the case without the locking nuts. Instead the centering gets, with some variability, better with each test

TABLE 5.1: X-axis and Y-axis extremes for each centering test

| Test (-) | X-axis (μm) | Y-axis (μm) |
|-------------|-----------------------------|-----------------------------|
| 1 | 62 | 66 |
| 2 | 66 | 70 |
| 3 | 58 | 62 |
| 4 | 66 | 64 |
| 5 | 60 | 64 |
| 6 | 60 | 58 |

Summarizing over 6 tests, the X-axis sees a reduction of displacement of $2 \mu\text{m}$, which corresponds to a 3.3 % decrease. Instead more interestingly the Y-axis has a stronger reduction of the displacement, $8 \mu\text{m}$, or 12.1 %. While the horizontal

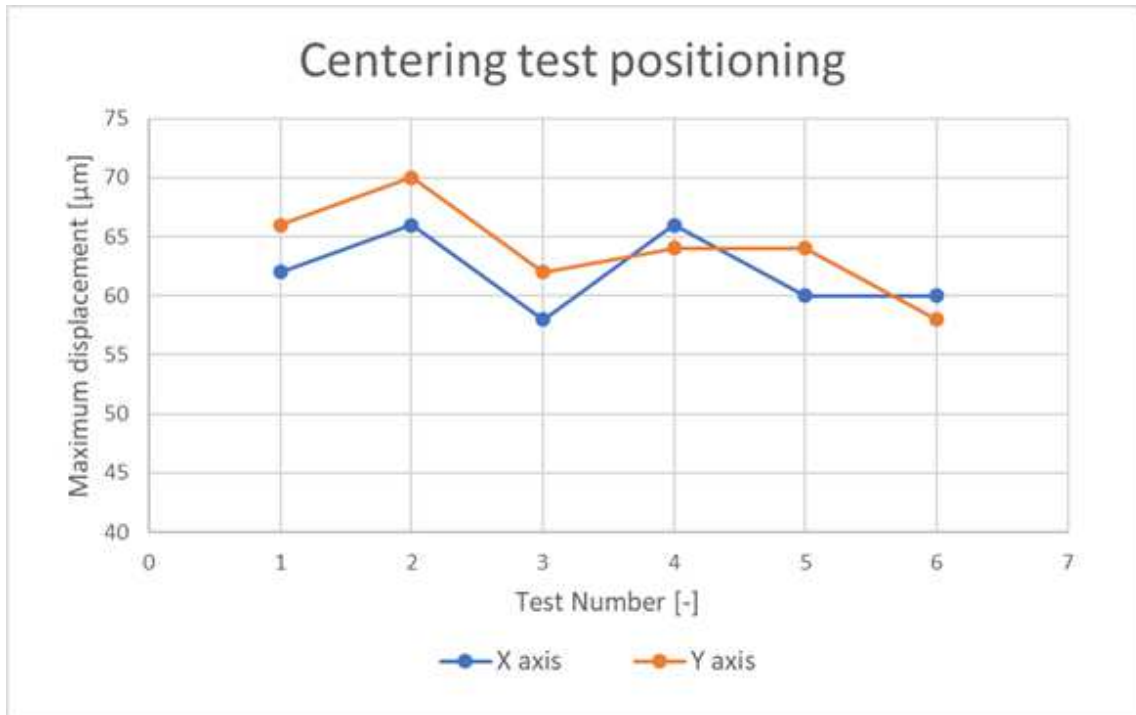


FIGURE 5.1: X-axis and Y-axis extremes for each centering test

movement can be considered basically constant, there is a much clearer trend of the vertical axis being more stable and centered with time. The Y-axis variability is 50 % more accentuated with respect to the X-axis one.

This condition could be due to the fact that, as the heavy duty tests go through, the primary bearing temperature get higher and higher and run more smoothly in the end with respect to the beginning of the test. This behavior happens even if a preheating process is applied to the machine before starting the tests. It is possible to feel directly that the shaft is easier to turn after the tests are performed.

A second reason of the variability of the data obtained is the axial positioning of the shaft. The locking rings on one right extreme of the shaft allow for few mm of movement of the shaft, and this possible variation can be one of the sources of the changing behavior of the centering.

As a last possible justification of the variability there is the way the holder plates lock onto the positioning screws. Considering the fact that the X-axis rotation forces are completely absorbed by the screw with the conical head, it is expected that the horizontal behavior is more stable. On the other hand the Y-axis is held

by the pressure exerted by the piston, so theoretically there is a less strong constraint imposed on the vertical direction.

5.2 Temperature behavior of the backup bearings

The analysis of the temperature measurement shows an interesting behavior of the bearing heat flow. The important temperatures with the different Δ in time are shown in Table 5.2 and Table 5.3, where T_0 is the initial temperature, T_{drop} is the temperature half a second before the drop down, Δ corresponds to the temperature increment from the start to the drop down, and from the drop down to T_{max} , which is the peak temperature reached during the drop down and subsequent cooling.

TABLE 5.2: Temperature change from start to drop down, without and with preheating

| | NO PREHEATING | | | PREHEATING | | |
|-----------|---------------|--------------------|---------------------------|---------------|--------------------|---------------------------|
| | T_0 (°C) | T_{drop} (°C) | $\Delta_{drop,0}$ (°C) | T_0 (°C) | T_{drop} (°C) | $\Delta_{drop,0}$ (°C) |
| A_lower | 22.4 | 22.8 | 0.4 | 23.4 | 25.0 | 1.6 |
| B_left | 22.4 | 22.8 | 0.4 | 23.6 | 25.2 | 1.6 |
| C_right | 22.4 | 22.8 | 0.4 | 23.6 | 25.1 | 1.5 |
| D_upper | 22.3 | 22.7 | 0.3 | 23.7 | 25.3 | 1.6 |
| E_support | 22.4 | 22.7 | 0.3 | 23.6 | 25.5 | 1.9 |
| F_env_in | 21.8 | 22.3 | 0.5 | 22.7 | 24.8 | 2.1 |
| G_env_out | 22.8 | 22.8 | 0.0 | 23.1 | 23.0 | -0.1 |

First of all it is clear that the temperature of the system depends on the preheating applied. Even if in the preheated case the machine was around 1.3 °C warmer with respect to the cold one, the heat transfer inside the safety glass is much stronger, causing a 1.6 °C raise across the internal sensors. In the cold test instead the temperature increase is limited to 0.4 °C.

The most interesting behavior are for sure the temperature change happening to the internal environmental data and the support one. As it is possible to see from Figure 4.14, the environmental sensor picks up a strong temperature change even if it is in a protected position from the direct wind coming from the motor. The support instead shows that it is much quicker at raising its temperature. This

TABLE 5.3: Temperature change from drop down to maximum temperature, without and with preheating

| | NO PREHEATING | | | PREHEATING | | |
|-----------|--------------------|-------------------|-----------------------------|--------------------|-------------------|-----------------------------|
| | T_{drop} (°C) | T_{max} (°C) | $\Delta_{max,drop}$ (°C) | T_{drop} (°C) | T_{max} (°C) | $\Delta_{max,drop}$ (°C) |
| A_lower | 22.8 | 23.7 | 0.9 | 25.0 | 26.1 | 1.1 |
| B_left | 22.8 | 23.8 | 1.0 | 25.2 | 26.5 | 1.3 |
| C_right | 22.8 | 23.9 | 1.1 | 25.1 | 26.8 | 1.7 |
| D_upper | 22.7 | 23.8 | 1.1 | 25.3 | 26.7 | 1.4 |
| E_support | 22.7 | 23.4 | 0.7 | 25.5 | 26.1 | 0.6 |
| F_env_in | 22.3 | 22.4 | 0.1 | 24.8 | 24.9 | 0.1 |
| G_env_out | 22.8 | 22.8 | 0.0 | 23.0 | 23.6 | 0.6 |

is to be expected, due to the large surface area of the component and its positioning directly near to the motor itself.

Considering the temperature increase during the acceleration phase, the preheated case presents a much stronger increase of the temperature. This is due to the fact that the air turbulence in the protective glass has time to move around and transfer as much thermal energy as it can to the support and to the bearing. It is also important to notice that, while the average increase of temperature in the components is around 1.6 °C, the environmental temperature inside increases of 2.1 °C.

Considering the reference temperature for the environment outside the protective plastic, it remains stable throughout the experiment up to some seconds after the drop down. Then a sudden spike happens and the temperature settles around 0.3 °C more with respect to before.

Another very interesting difference is the temperature change between drop down and maximum. Even if the shaft stays in contact for the same time with the bearing, the increase is much stronger in the preheated case, passing from an average on the bearing ring of 1.0 °C increase in the cold machine case to a 1.4 °C increase in the second case. This is even more important because the machine was in a hotter state in the second experiment, so the thermal dissipation to the environment is working against the spike of temperature. Most likely the temperature difference is due to the fact that the shaft is warmer in the second case, and the temperature increase is not only due to the friction between shaft and the bearing, as well as the internal bearing friction, but also due to some direct conduction happening in the few seconds of contact.

Since all the temperature are more or less in the same range and order of magnitude, it is possible to be conservative and consider an uncertainty on each value of 0.4 °C.

Chapter 6

Summary

The AMB³ test bench as it was in the initial condition had some issues in its working condition. The maximum speed was not satisfactory with respect to the design condition, the centering was not properly holding and there was not any possibility to collect the temperature data from the backup bearings. Moreover there were some problems related to a set of backup bearings, which were damaged by most likely dirt.

Regarding the speed limitation, with the modification of the lower holder plate locking bolt and the addition of locking nuts to the positioning screws, now the system is capable to reach 28000 rpm and work as it was designed for. The vibrations happening during the acceleration phase, especially around 10500 shaft rpm (1100 motor rpm), do not cause anymore the loss of positioning on the holder plates, so the system can be used safely and efficiently.

Considering the temperature measurement system, it is now setup and ready to use whenever needed. Since it is not directly integrated on the ABB automation builder, but it is developed in LabView[™], some attention is needed to properly couple the temperature data with the speed data coming from the pre-existing software. The data allows to have a full characterization of the thermal gradient present on the backup bearing after each drop down test. Some environmental data are also recorded in and out of the safety glass to have a better knowledge of the state of the system. The temperature measurement must be activated manually since, as said before, it was developed out of the ABB environment, due to some problems with the software licensing.

The damaged backup bearings are substituted and ready to work again at the best condition. Since it was not possible to install some bearings caps during the

thesis work, it is suggested a quick addition of them, in case of heavy use of the machine.

Bibliography

- [1] R. Viitala, I. Tätilä, R. Aho, P. Kiviluoma, A. Korhonen, and P. Kuosmanen. "Backup bearing testing device for active magnetic bearing". In: *11th International DAAAM Baltic Conference "INDUSTRIAL ENGINEERING"* (2016).
- [2] Meirovitch Leonard. *Fundamentals of Vibrations*. McGraw-Hill, 2001.
- [3] Kjaer Bruel. *Measuring Vibration*. K Larson and Son, 1982.
- [4] Chetan P. Chaudhari, Bhushan B. Thakare, Saurabh R. Patil, and Shrikant U. Gunjal. "A STUDY OF BEARING AND ITS TYPES". In: *International Journal of Advance Research In Science And Engineering* (2015).
- [5] Wlodzimierz Bryc. *The Normal Distribution: Characterizations with Applications*. Springer Science & Business Media, 2012.
- [6] Tempsens. *Temperature Hand Book*. Tempsens Instruments, 2006.
- [7] *Lead compensation techniques for RTDs*. <http://www.defineinstruments.com/blog/lead-compensation-techniques-for-rtDs>. Accessed: 2018-05-20.
- [8] International Electrotechnical Commission. "Industrial platinum resistance thermometers and platinum temperature sensors". In: (2008).

Appendix 1

Appendix: MATLAB® scripts

In this Appendix the parts of MATLAB® code used for the plot creation and the data fetching from the ABB system.

MATLAB® SCRIPT FOR THE CREATION OF THE DIRECTORY

```
1 %% Hae_mittausdata
2
3 cd('C:\Users\mittaaja\Documents\MATLAB')
4
5 date = datestr(now, 'yyyymmddTHHMMSS')
6
7 outputdir = strcat('Mittausdata/mittaus_', date)
8
9 dos('ftpget MITTAUS.ZIP')
10
11 unzip('MITTAUS.ZIP', outputdir)
12
13 cd('Mittausdata');
14
15 run('Wav_read_ver6.m');
16
17 cd('../');
```

MATLAB® SCRIPT FOR THE PLOT CREATION

```
1 clc
```

```
2 close all
3 volcalc=0.00000238418579101562;
4 %Calculation constant for converting analog channel value
  to volts
5
6 mittaus = strcat('mittaus_', date);
7 cd(mittaus);
8
9 filename1=strcat(mittaus, '/CH00_ENA.wav');
10 fileid1=fopen(filename1, 'r', 'b');
11 filecontent1=fread(fileid1, 'int32');
12 data1=filecontent1(12:end);
13 volt1=data1*volcalc;
14
15 filename2=strcat(mittaus, '/CH01_nEN.wav');
16 fileid2=fopen(filename2, 'r', 'b');
17 filecontent2=fread(fileid2, 'int32');
18 data2=filecontent2(12:end);
19 volt2=data2*volcalc;
20
21 filename3=strcat(mittaus, '/ENCODE_A.wav');
22 fileid3=fopen(filename3, 'r', 'b');
23 filecontent3=fread(fileid3, 'int32');
24 data3=filecontent3(12:end);
25 revcount=data3;
26
27
28 fclose('all');
29 t=linspace(0,(length(data1)/12500),length(data1));
30
31 hold on
32
33 %xy-plot
34 subplot(5,2,[1,4]);
35 plot(volt1/10, volt2/10, 'r');
36 axis([0 1 0 1], 'equal');
37 title(strcat('xy-plot of the center point for ',date));
38 ylabel('y position [mm]');
39 xlabel('x position [mm]');
40 grid on
41 grid minor
42
```

```
43 subplot(5,2,[5,8]);
44 volt1a=volt1-mean(volt1);
45 volt2a=volt2-mean(volt2);
46 plot (volt1a*100, volt2a*100, 'r');
47 axis('equal');
48 ylabel('y position [\num]');
49 xlabel('x position [\num]');
50 grid on
51 grid minor
52
53 %tx-plot
54 subplot(5,2,9);
55 plot (t, volt1, 'b');
56 axis([0 t(end) 0 24]);
57 title('x-coordinate in time');
58 xlabel('Time [s]');
59 grid on
60 grid minor
61
62 %ty-plot
63 subplot(5,2,10);
64 plot (t, volt2, 'g');
65 axis([0 t(end) 0 24]);
66 title('y-coordinate in time');
67 xlabel('Time [s]');
68 grid on
69 grid minor
70 hold off
71
72
73 % save figure
74 savefig(mittaus);
75
76 % calculate rpm
77 up = find(diff(revcount)~=0);
78 i = 1;
79 revs = length(up);
80 ticsperrev = zeros(revs,1);
81 while i < revs
82     ticsperrev(i) = up(i+1)-up(i);
83     i = i+1;
84 end
```

```
85
86 rpm = zeros(length(revcount),1);
87 %rpm(1:up(1)) = 0;
88 i = 1;
89 while i < revs-1
90     x = 1*((12500*60)/ticsperrev(i));
91     rpm(up(i)+1:up(i+1)) = x;
92
93     i = i+1;
94 end
95
96
97 % plot rpm
98 figure;
99 plot (t, rpm, 'k');
100 %axis([0 t(end) -24 0]);
101 title('rpm in time');
102 grid on
103 grid minor
104 xlabel('Time [s]');
105 savefig(strcat('rpm_',mittaus));
106
107 % plot rpm, x and y
108 figure;
109 subplot(3,1,1);
110 plot (t, volt2, 'g');
111 title('y-coordinate in time');
112 grid on
113 grid minor
114 subplot(3,1,2);
115 plot (t, rpm, 'k');
116 title('rpm in time');
117 grid on
118 grid minor
119 subplot(3,1,3);
120 plot (t, volt1, 'b');
121 title('x-coordinate in time');
122 grid on
123 grid minor
124 xlabel('Time [s]');
125 savefig(strcat('rpm_x_y_',mittaus));
126
```

```
127 % xy-plot
128 figure;
129 volt1a=volt1-mean(volt1);
130 volt2a=volt2-mean(volt2);
131 plot (volt1a*100, volt2a*100, 'r');
132 axis('equal');
133 ylabel('y position [\num]');
134 xlabel('x position [\num]');
135 grid on
136 grid minor
137 savefig(strcat('xy_',mittaus));
138
139
140 % figure;
141 % plot (t, volt2, 'g');
142 % axis([0 t(end) 0 24]);
143 % title('y-coordinate in time, microepsilon');
144 % grid on
```


Appendix 2

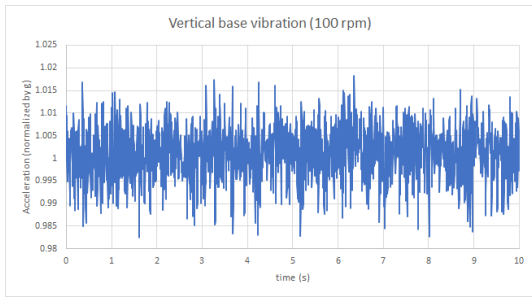
Appendix: Vibration data

In this Appendix, the data obtained by the vibration analysis is presented in graphical form, after Table 2.1, which synthesizes the results obtained in Figure 4.1.

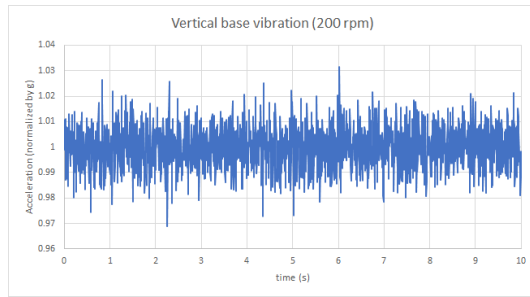
The average column is computed with Formula 2.1, the Standard deviation is computed with Formula 2.2. Max and Min columns are computed by considering a 99 % confidence level, so by summing (Max) and subtracting (Min) to the average the standard deviation multiplied by the value 2.58 from Table 2.1.

| Motor speed (rpm) | Average (g) | Standard deviation (g) | Max (g, 99% CL) | Min (g, 99% CL) |
|------------------------------|------------------------|-----------------------------------|----------------------------|----------------------------|
| 100 | 1.00105 | 0.00570 | 1.016 | 0.986 |
| 200 | 0.99987 | 0.00815 | 1.021 | 0.979 |
| 300 | 1.00074 | 0.01721 | 1.045 | 0.956 |
| 400 | 1.00060 | 0.01854 | 1.048 | 0.953 |
| 500 | 1.00184 | 0.01574 | 1.042 | 0.961 |
| 600 | 0.99957 | 0.01860 | 1.047 | 0.952 |
| 700 | 0.99855 | 0.02810 | 1.071 | 0.926 |
| 800 | 1.00417 | 0.03188 | 1.086 | 0.922 |
| 900 | 1.00329 | 0.03162 | 1.085 | 0.922 |
| 1000 | 1.00277 | 0.08445 | 1.220 | 0.785 |
| 1100 | 1.00866 | 0.79688 | 3.061 | -1.044 |
| 1200 | 0.99946 | 0.12048 | 1.310 | 0.689 |
| 1300 | 1.00572 | 0.14338 | 1.375 | 0.636 |
| 1400 | 1.01232 | 0.20336 | 1.536 | 0.488 |
| 1500 | 1.00438 | 0.31579 | 1.818 | 0.191 |
| 1600 | 1.00347 | 0.14126 | 1.367 | 0.640 |
| 1700 | 1.00337 | 0.13612 | 1.354 | 0.653 |
| 1800 | 0.99541 | 0.10255 | 1.260 | 0.731 |
| 1900 | 1.00152 | 0.15482 | 1.400 | 0.603 |
| 2000 | 1.00130 | 0.12547 | 1.325 | 0.678 |
| 2100 | 1.00423 | 0.13379 | 1.349 | 0.660 |
| 2200 | 1.00177 | 0.13023 | 1.337 | 0.666 |
| 2300 | 1.00263 | 0.08066 | 1.210 | 0.795 |
| 2400 | 1.00307 | 0.09578 | 1.250 | 0.756 |
| 2500 | 1.00417 | 0.09422 | 1.247 | 0.761 |
| 2600 | 1.00120 | 0.11876 | 1.307 | 0.695 |
| 2700 | 1.00133 | 0.18220 | 1.471 | 0.532 |
| 2800 | 1.02225 | 0.21114 | 1.566 | 0.478 |
| 2900 | 1.00531 | 0.16488 | 1.430 | 0.581 |
| 3000 | 1.00111 | 0.19507 | 1.504 | 0.499 |

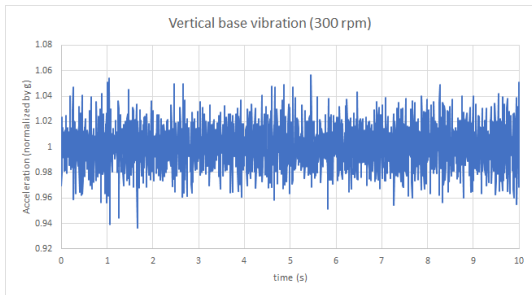
TABLE 2.1: Summary of the main results for the vibration analysis



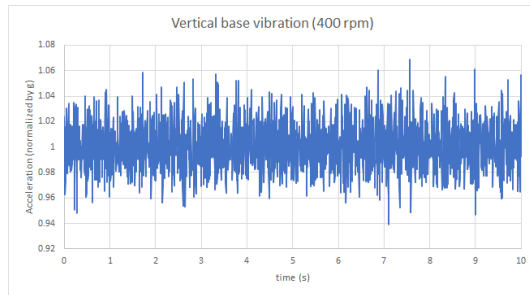
100 motor rpm vibration



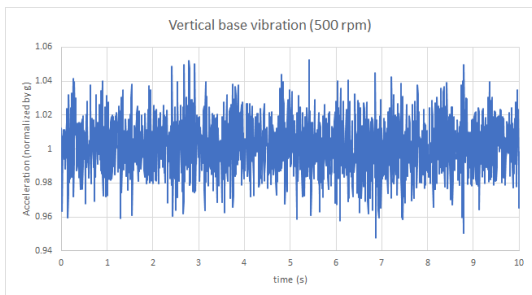
200 motor rpm vibration



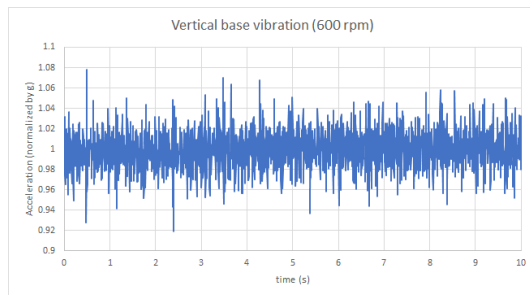
300 motor rpm vibration



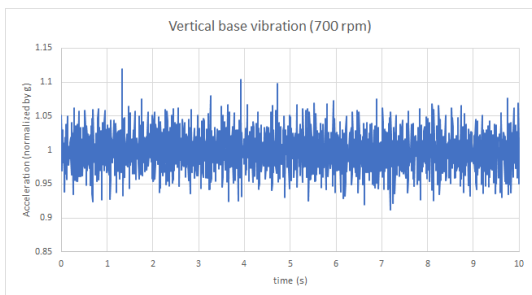
400 motor rpm vibration



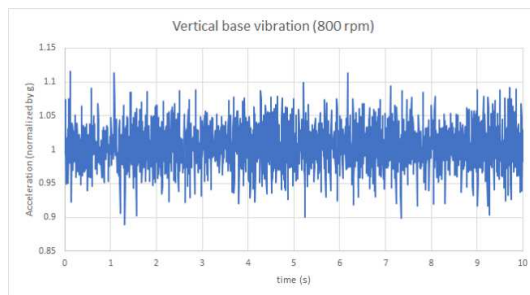
500 motor rpm vibration



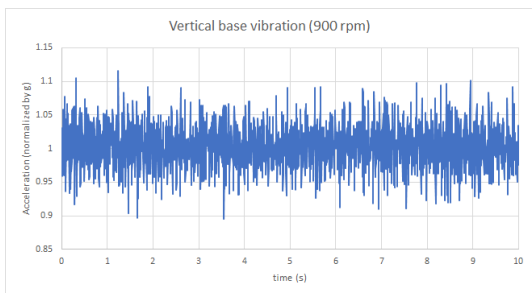
600 motor rpm vibration



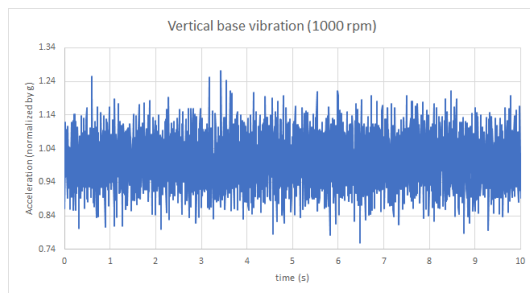
700 motor rpm vibration



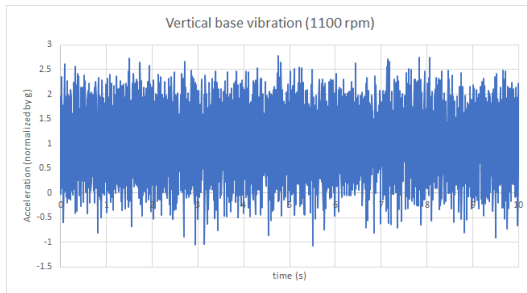
800 motor rpm vibration



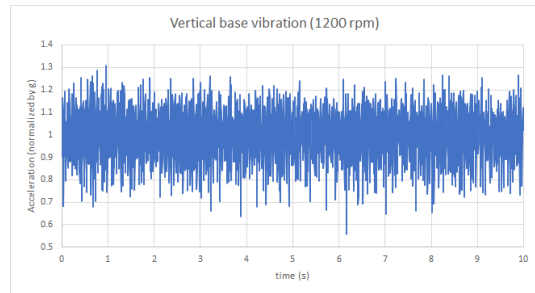
900 motor rpm vibration



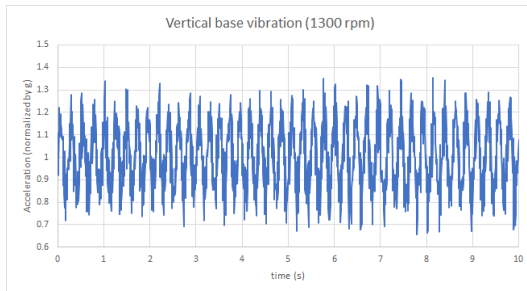
1000 motor rpm vibration



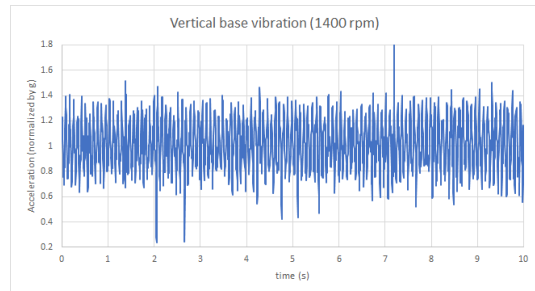
1100 motor rpm vibration



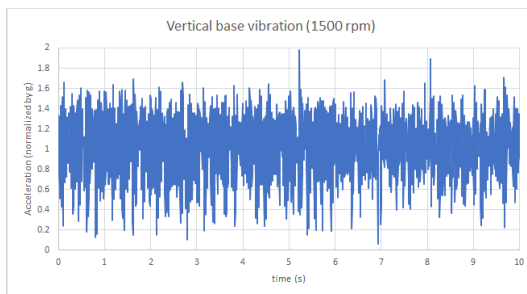
1200 motor rpm vibration



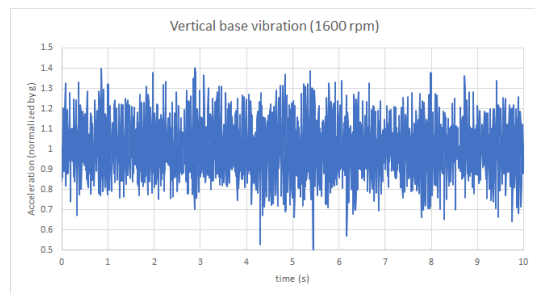
1300 motor rpm vibration



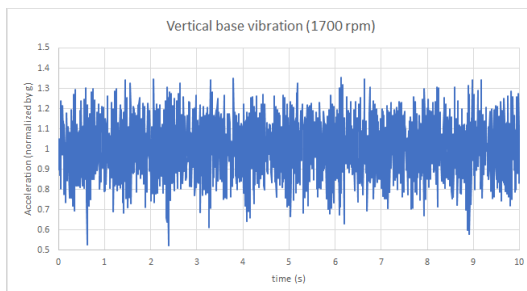
1400 motor rpm vibration



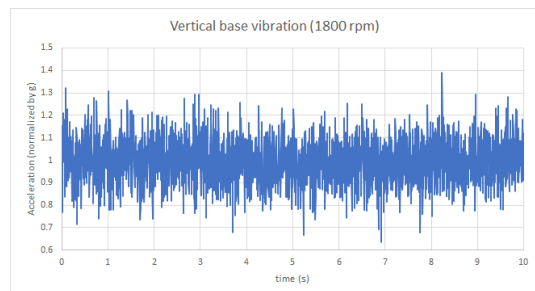
1500 motor rpm vibration



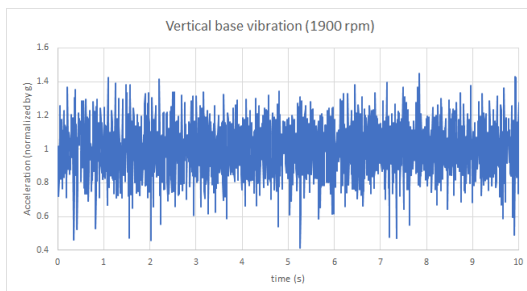
1600 motor rpm vibration



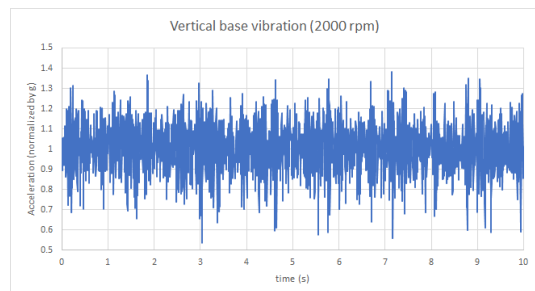
1700 motor rpm vibration



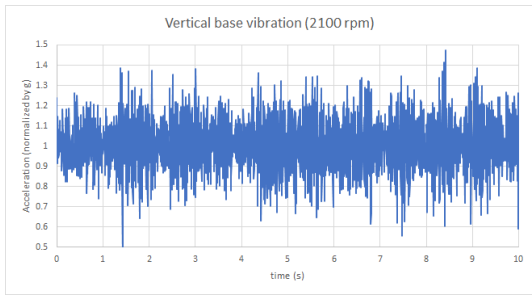
1800 motor rpm vibration



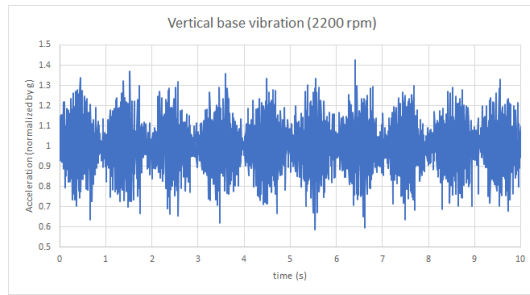
1900 motor rpm vibration



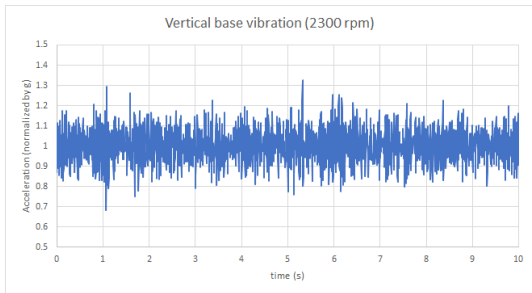
2000 motor rpm vibration



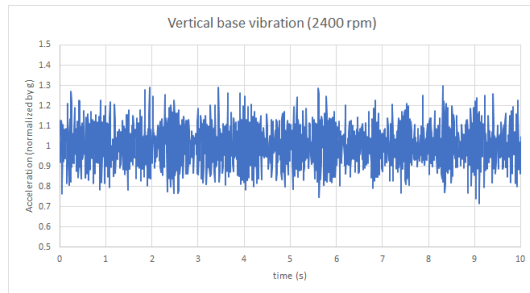
2100 motor rpm vibration



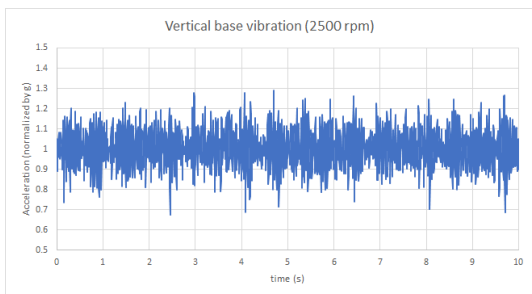
2200 motor rpm vibration



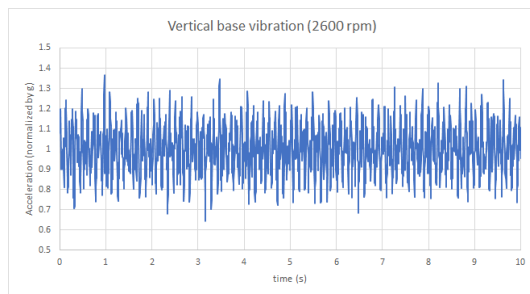
2300 motor rpm vibration



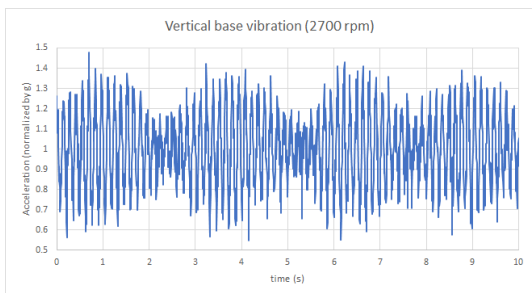
2400 motor rpm vibration



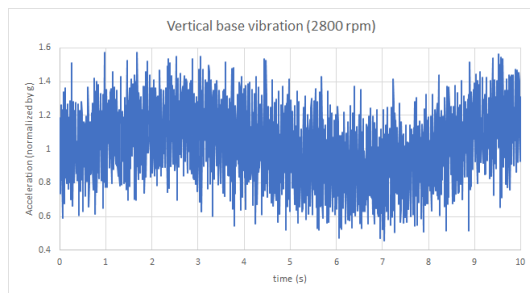
2500 motor rpm vibration



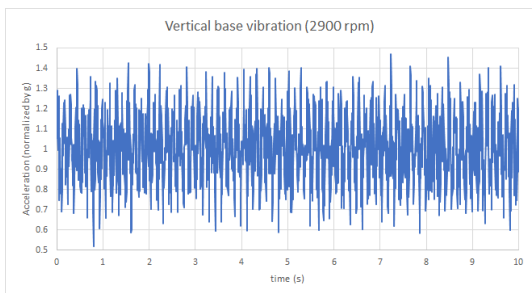
2600 motor rpm vibration



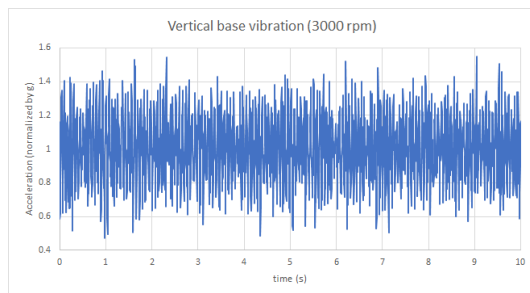
2700 motor rpm vibration



2800 motor rpm vibration



2900 motor rpm vibration



3000 motor rpm vibration

Appendix 3

Appendix: Drop down and centering test

In this Appendix, the complete output of the centering and the drop down tests is presented.

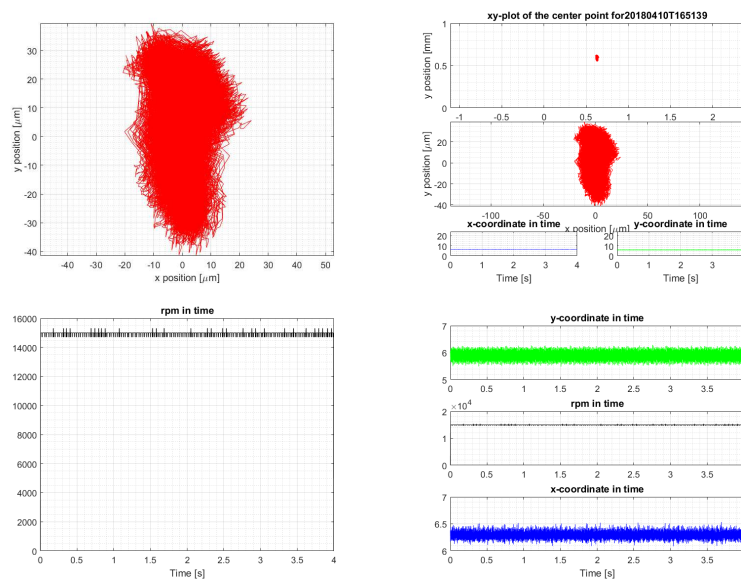


FIGURE 3.1: Centering test 1 without locking nuts

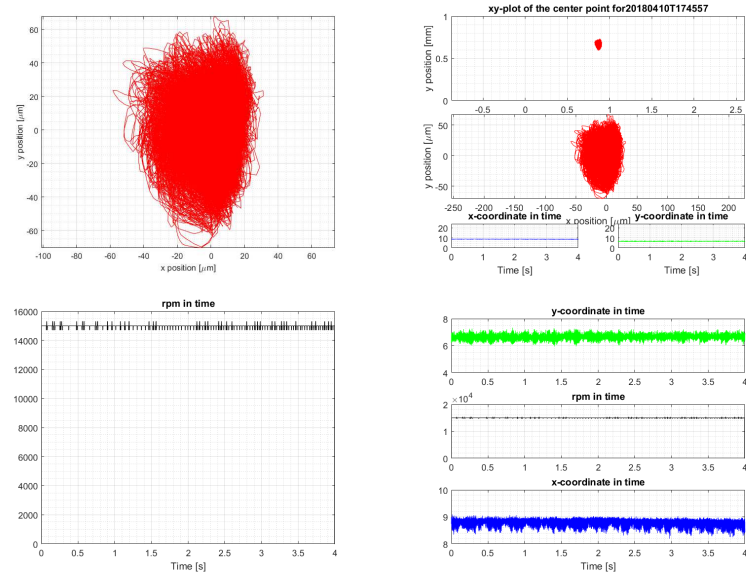


FIGURE 3.2: Centering test 2 without locking nuts

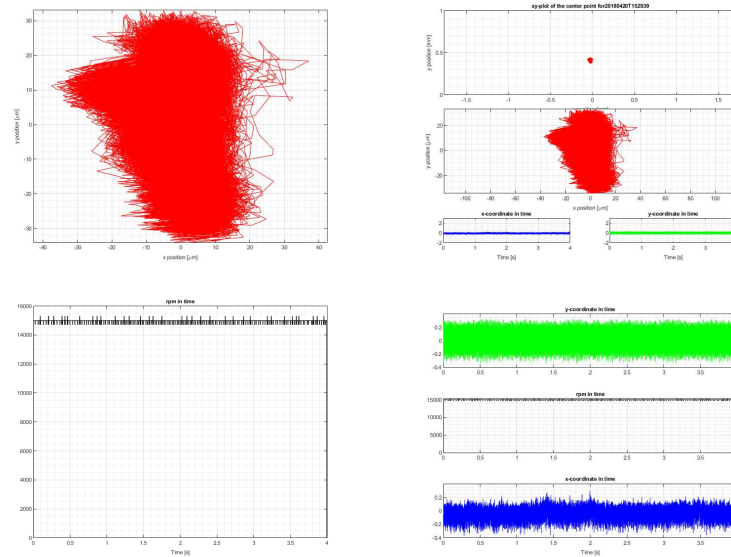


FIGURE 3.3: Centering test 1 with locking nuts

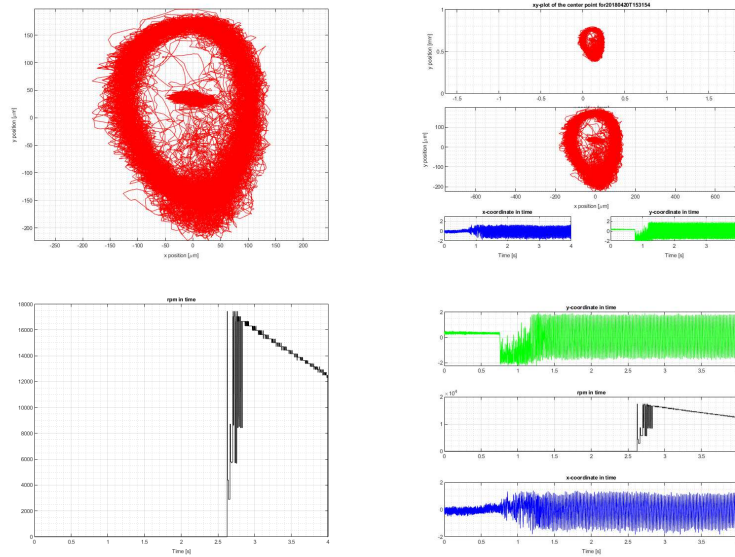


FIGURE 3.4: Dropdown test 1 with locking nuts

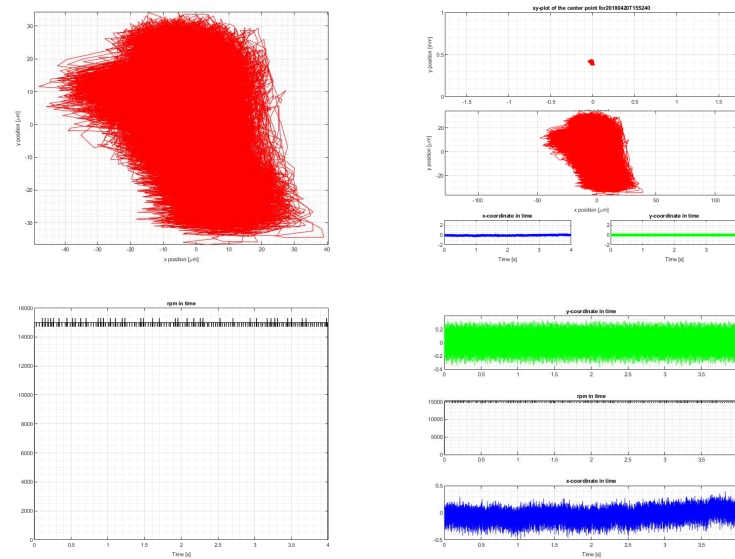


FIGURE 3.5: Centering test 2 with locking nuts

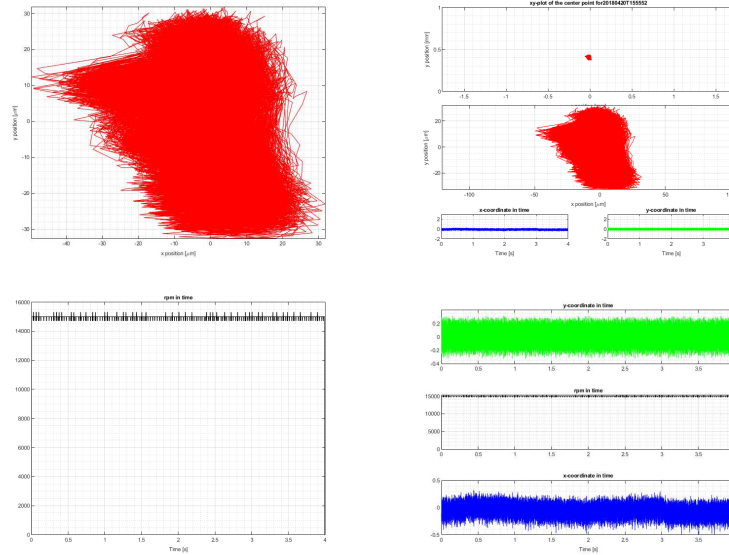


FIGURE 3.6: Centering test 3 with locking nuts

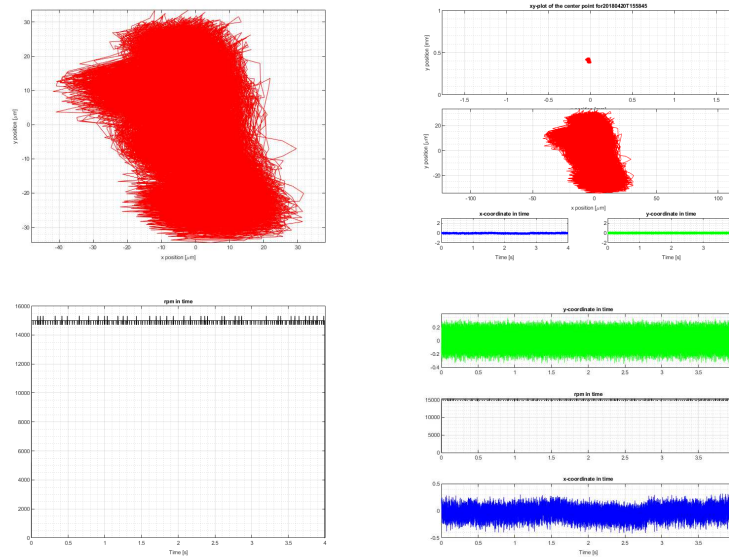


FIGURE 3.7: Centering test 4 with locking nuts

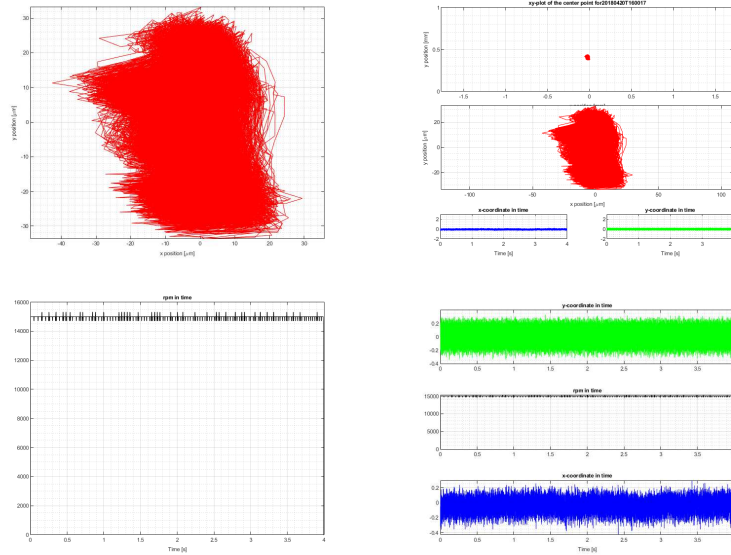


FIGURE 3.8: Centering test 5 with locking nuts

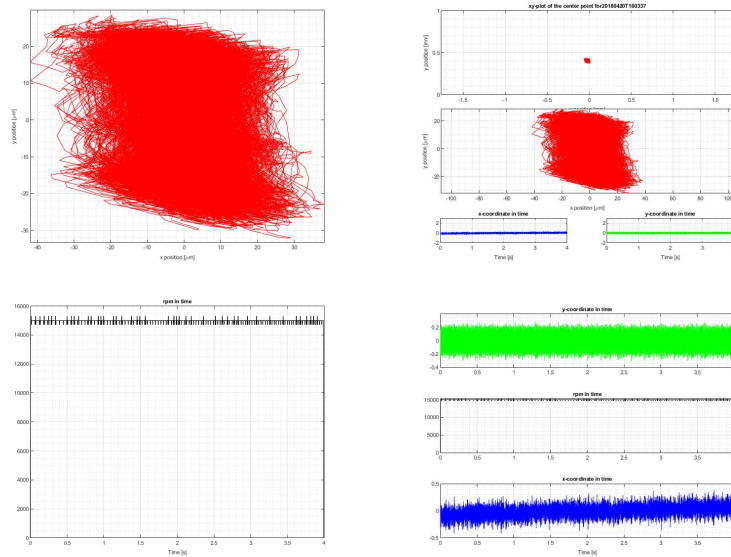


FIGURE 3.9: Centering test 6 with locking nuts

Appendix 4

Appendix: Abstract from Aalto University

Author Michele Tunesi

Title of thesis BACKUP BEARING TEST BENCH UPGRADE AND EVALUATION

Master program Mechanical engineering

Thesis supervisor Professor Petri Kuosmanen, Professor Eugenio Brusa

Thesis advisor(s) M. Sc Raine Viitala

Date 11.05.2018**Number of pages** 69**Language** English

Abstract

Safety of the machines and evaluation of backup systems is fundamental for the industry to develop a secure environment for the employee and ensure that components do not get damaged in case of a failure. Having the possibility to test the behavior of a bearing under the extreme stress of a simulated failure scenario is an important capability that allows to practically test these complex components. The test bench aims to characterize the behavior of the shaft when drop down at high speed on a backup bearing set. The machine was developed and designed to have a high rpm speed of test and quick maintenance and calibration.

The aim of the study was to start on the solid design previously done and improve it to extend its capabilities and to fix some of the calibration and operational problems that became evident with time. The system was designed to withstand rpm up to 28'000, and the screw positioning system was fixed to obtain that. The vibration during acceleration were quite large, in the order of the hundreds of μm , and now thanks to the screw system and the lower holder plate modification are reduced in the order of the tens of μm . As a further expansion of the capabilities, a measurement system for the temperature was added on one side of the machine to record the temperature on the outer ring of the bearing.

The main result was that the machine now is capable of reliably perform the tests without interruption and with no need of recalibration between each test. The centering remains stable through the measurement runs. The temperature measurement system is set up and ready to record data. Some initial test showed an interesting gradient of temperature in time toward the higher part of the bearing, exactly on the opposite side of where the shaft is dropped.

Keywords Backup bearing, Testing, Safety, Temperature measurement
